The origin and occurrence of subaqueous sedimentary cracks

SEAN McMAHON[1]*, ASHLEIGH VAN SMEERDIJK HOOD[1] & DUNCAN McILROY[2]

[1]*Department of Geology and Geophysics, Yale University, 210 Whitney Avenue, New Haven, CT 06511, USA*

[2]*Department of Earth Sciences, Memorial University of Newfoundland, St John's, NL, A1B 3X5, Canada*

**Correspondence: sean.mcmahon@yale.edu*

Abstract: The rock record attests that sediments have cracked at or below the sediment–water interface in strictly subaqueous settings throughout Earth history. In recent decades, a number of hypotheses have been advanced to explain this phenomenon, but these are widely regarded as being mutually exclusive and there is little consensus about which model is correct. In this paper, we first review the geometries, lithologies and range of facies in which subaqueous sedimentary cracks occur in the geological record, with particular attention to cracks in carbonates. We then evaluate current models for subaqueous cracking, emphasizing that different models may be correct with respect to different sets of cracks, but that cracking is generally a two-step process involving sediment stabilization prior to disruption. We also present the results of some simple new experiments designed to test the dominant models of crack formation. These results demonstrate for the first time that microbial mats can produce thin, shallow cracks at the sediment–water interface. We conclude that the presence of cracks in marine, brackish and lacustrine rocks should not be used uncritically to infer fluctuations in salinity in the depositional environment.

Supplementary material: A video showing a micro-CT scan of a hand-sample from the Monteville Formation, South Africa is available at https://doi.org/10.6084/m9.figshare.c.3580673

Marine and lacustrine rocks throughout the geological record preserve cracks demonstrably opened in soft substrates at or below the sediment–water interface, without any possibility of desiccation. Here, we reserve the term 'crack' for originally sharp-walled, approximately planar cavities formed predominantly by brittle failure rather than fluid interpenetration or dissolution. Most are filled either by sediment or by authigenic minerals and superficially resemble desiccation cracks, although they typically lack mud curls (Tanner 2003). This resemblance has tempted some researchers to suggest that subaqueous cracking, like sub-aerial cracking, has a single universally applicable explanation (e.g. Pratt 1998*a*), whereas others have explicitly rejected this assumption (Davies *et al.* 2016). The most widely cited models invoke shrinkage due to the expulsion of water from swelling clays or flocculating particles, either as a result of salinity changes, gravitational compaction or seismic disturbance (Burst 1965; Plummer & Gostin 1981; Pratt 1998*a*). In recent decades, several occurrences have been attributed to the effects of microbial biostabilization (e.g. Pflueger 1999; Gehling 2000; Harazim *et al.* 2013). Each of these explanations may be correct, or partially correct, in particular contexts. However, because many workers assume a gel dewatering (synaeresis) origin for subaqueous cracks (e.g. Fairchild 1980; Carroll & Wartes 2003; Bhattacharya & MacEachern 2009; Buatois *et al.* 2011) – and also because it has become a conventional descriptive term uncritically used for all non-desiccation cracks – the term 'synaeresis crack' retains wide currency. Harazim *et al.* (2013) preferred 'intrastratal shrinkage crack' as a more neutral alternative, which is appropriate for cracks that form by sediment shrinkage below the sediment–water interface. Here, we use the broader term 'subaqueous sedimentary cracks' to avoid implying either a causative mechanism or a position with respect to the sediment–water interface.

Subaqueous cracks in the rock record

Subaqueous sedimentary cracks representing a wide range of ages, morphologies, sediment compositions and palaeoenvironments have been documented (Table 1). Occurrences have been reported from marine, marginal, lacustrine and fluvial depositional environments, with a possible shoaling trend

From: Brasier, A. T., McIlroy, D. & McLoughlin, N. (eds) 2017. *Earth System Evolution and Early Life: A Celebration of the Work of Martin Brasier*. Geological Society, London, Special Publications, **448**, 285–309.
First published online November 30, 2016, https://doi.org/10.1144/SP448.15

Table 1. *Occurrence of subaqueous sedimentary cracks in the geological record*

Stratigraphy/ location	Age	Shape	Host lithology	Infill	CO_3	MISS	Inferred setting	Reference
Kauai, Hawaii	Quaternary	P: semi-polygonal	Carbonate speleothems in basalt	None	✓	✓	Speleothem	Lévéille *et al.* (2000)
West Basin Lake, Victoria, Australia	Quaternary	V: jagged, curved	Aragonite, dolomite, hydromagnesite	Void space; carbonate cements	✓	✓	Lacustrine	Van Leeuwen (2013); field observations
Green River Fm, Wyoming, USA	Eocene	V: ptygmatic	Siltstone–carbonate–mudstone	Carbonate mud/ silt	✓	ND	Sublittoral	Törö *et al.* (2013)
Xialiao Basin, China	Palaeogene	V: ptygmatic	Mudstone	Sand	✖	✖	Lacustrine/ swamp	Hsiao *et al.* (2010)
Cujupe Fm, Brazil	Cretaceous–Palaeogene	P: polygonal	Mudstone (with interbedded sandstone)	ND	✖	ND	Estuarine/ bay (*)	Rossetti (1998)
Austral Basin, Argentina	Late Cretaceous	V: ptygmatic	Mudstone	Sand	✖	ND	Fluvio-deltaic	Buatois *et al.* (2011)
Dunvegan Fm, Alberta, Canada	Cretaceous	V: ptygmatic spindles	Mudstone	Silt–fine sand	ND	ND	Fluvio-deltaic	Bhattacharya & MacEachern (2009)
Dunga oilfield, Kazakhstan	Cretaceous	V: V-shaped, branching downwards	Black heterolithic sandstone	Sand	✓	✖	Shoreface/ deltaic (*)	Cazier *et al.* (2011)
Raimalro Lst., Kuar Bet Mb, India	Middle Jurassic	P: curlicue	Micritic sandstone	Calcite	✓	✖	Marine	Patel *et al.* (2013)
Lockatong Fm, New Jersey/ Philadelphia, USA	Triassic	P: sinuous	Calcareous siltstone	Analcime, dolomite	✓	ND	Lacustrine	Van Houten (1962)
Liard Fm, British Columbia, Canada	Middle Triassic	V: vertical spindles	Dolomitic mudstone/ sandstone	ND	✓	✓	Lagoonal	Zonneveld *et al.* (2001)
Lucaogou Fm, NW China	Late Permian	V: branching spindles	Dolomitic mudstone		✓	ND	Lacustrine	Carroll & Wartes (2003)

Pebbley Beach Fm, New South Wales, Australia	Early Permian	V: ptygmatic, V-shaped	Carbonaceous mudstone	Carbonaceous	✖	ND	Estuarine/deltaic	Fielding *et al.* (2006)
Orcadian Basin, UK	Devonian	P: bird's foot, spindles V: ptygmatic	Shale	Coarse silt	✓	ND	Lacustrine	Donovan & Foster (1972)
Murzuk Basin, Libya	Silurian	P: bird's foot, sinuous, curlicue, rectangular	Sandstone and (inferred) mudstone	Sand	ND	✓	Shallow marine	Pflueger (1999)
Beach Fm, Newfoundland, Canada	Early Ordovician	V: ptygmatic	Shale	Sand	✖	✓	Marine	Harazim *et al.* (2013)
Petit Jardin, Berry Head Fms, Newfoundland, Canada	Late Cambrian	V: straight, jagged, pinching and swelling, branching downwards	Dolomitic mudstone–oolite	Mud chips and ooids, calcite spar, fine dolomite cement	✓	✖	Shallow marine	Cowan & James (1992)
Gushan and Chaomidian Fms, China	Late Cambrian	P: reticulate V: vertical	Thin limestone interbeds	Dolomitic marlstone	✓	✖	Shallow carbonate platform	Chen *et al.* (2009)
St Lawrence Fm, Mississippi Valley, USA	Late Cambrian	P: isolated curving spindles V: ptygmatic spindles	Fine dolomitic argillite	Sand	✓	Kinneyia	Marine	Hughes & Hesselbo (1997)
Reno Mb, Lone Rock Fm, Wisconsin, USA	Late Cambrian	P: spindles forming partial polygons	Thin clay-bearing sandstone	ND	✖	✓	Marine	Eoff (2014)
Hales Limestone case study, Nevada, USA	Late Ordovican–Early Cambrian	P: polygonal V: V-shaped	Calcareous shale	Calcite spar	✓	✖	Marine slope	Cook & Taylor (1977); this paper
Bonahaven Fm, Mb 3	Neoproterozoic	P: spindles; incomplete polygons V: ptygmatic	Dolostone, silty dolomite	Sand	✓	✖	Shallow subtidal	Fairchild (1980)
Bonahaven Fm, UK	Neoproterozoic	P: curving, quasi-polygonal V: V-shaped, branching, with flaring of host layers	Sandstone	Sand	ND	✖	Intertidal/shallow marine	Tanner (1998)

(*Continued*)

Table 1. *Occurrence of subaqueous sedimentary cracks in the geological record* (*Continued*)

Stratigraphy/ location	Age	Shape	Host lithology	Infill	CO_3	MISS	Inferred setting	Reference
Irby Siltstone, Tasmania, Australia	Neoproterozoic	V: Ptygmatic, tapered	Dolostone	Dolospar, silt	✓	ND	Low energy, marine	Calver & Baillie (1990)
Brachina Fm, ABC Range Quartzite, South Australia	Ediacaran	P: Isolated spindles	Mudstone	Sand, silt	✖	ND	Shallow marine	Plummer & Gostin (1981)
Masirah Bay Fm, Oman	Ediacaran	V: Branching spindles and incomplete polygons	Sandstone (70–80% quartz)	Sandstone	✖	✖	Shallow marine–shoreface	Allen & Leather (2006)
Nuccaleena Fm, South Australia	Ediacaran	Sheet cavities, straight to curved	Dolomite	Dolomite marine cements, spar	✓	✖	Deep marine	Field observations
Keilberg Mb, Namibia	Ediacaran	Sheet cavities, straight to curved	Dolomite	Dolomite marine cements	✓	✖	Deep marine	Hoffman & Macdonald (2010); field observations
Ediacara Mb, South Australia	Ediacaran	P: sinuous and polygonal	Sandstone	Sand	✖	✓	Marine	Gehling (2000)
Balcanoona Fm, South Australia	Cryogenian	Sheet cavities, cemented	Dolomite	Dolomite marine cements, spar	✓	✖	Marine platform	Field observations
Gauss Fm, Namibia	Cryogenian	Sheet cavities, straight to curved, ptygmatic	Dolomite	Dolomite marine cements, spar	✓	✓	Marine platform	Field observations
Trezona Fm, South Australia	Cryogenian	P: spindle, curved	Limestone	Sparry calcite, aragonite cements, ferruginous mud	✓	✓	Marine	De Morton (2011), field observations
Elbobreen Fm, Spitsbergen	Cryogenian	V: ptymagtic spindles and disjointed ribbons	Limestone	Calcite microspar	✓	✓	Shallow marine (*lagoon?)	Fairchild & Hambrey (1984) (molar tooth in Halverson *et al.* 2004)
Kitwe Fm, Zambia	Tonian	P: bird's foot	Dolomitic/ siliciclastic	Dolomite/ anhydrite	✓	✓	Intertidal/ lacustrine	Clemmey (1978) (disputed by Porada & Druschel 2010)

Beck Spring Dolomite, California, USA	Tonian	V: linear to ptygmatic	Dolomite	Layered mudstone	✓	✓	Shallow marine	Harwood & Sumner (2011)
Devede Fm, Namibia	Tonian	P: sinuous/linear V: tapered/spindles	Dolomite	Dolomite marine cements, spar	✓	✓	Shallow marine	Hood *et al.* (2015)
Little Dal Group, Northwest Territories, Canada	Tonian	V: ptygmatic molar tooth	Lime mudstone	Sparry calcite	✓	✓	Marine platform	Turner *et al.* (1997)
Chuanlinggou Shale, north China	Mesoproterozoic	V: ptygmatic	Black shale	Fine sand	✓	✓	Marine	Xiaoying *et al.* (2008)
Chhatisgarh Fm, India	Mesoproterozoic	P: sinusoidal to spindle	Medium quartz arenite	ND	✖	✓	Shallow nearshore marine	Chakraborty *et al.* (2012)
Libby Fm, Minnesota, USA	Mesoproterozoic	P: spindles, incomplete polygons V: V-shaped, bulging, ptygmatic	Silty mudstone	Coarse silt, sand	✖	✓	Deltaic mudflat	Kidder (1990)
Belt Supergroup, Minnesota, USA/Canada	Mesoproterozoic	V: ptygmatic, curved, molar tooth	Micritic dolostone, limestone	Calcite microspar	✓	ND	Marine	Horodyski (1976); Pratt 1998a, b; Frank & Lyons (1998)
Appekunny Fm (Belt Supergroup), Minnesota, USA/Canada	Mesoproterozoic	P: sinusoidal. V: jagged, sigmoidal, curved, straight, ptygmatic	Sandstone, siltstone, shale	Sand, mud chips	✖	✖	Marine	Pratt 1998a, b
Uncompahgre Group, Colorado, USA	Early Proterozoic	P: ptygmatic, curved	Mudstone	Sand	✖	✖	Marine shelf	Harris & Eriksson (1990)
Gunflint Fm, Ontario, Canada	Palaeoproterozoic	P: tapering, radio-concentric	Granular iron formation (chert)	Quartz	✖	ND	Marine	Jirsa & Fralick (2010)

*Setting inferred partially from interpretation of cracks as evidence of fluctuating salinity.
This is a non-exhaustive list of examples, selected from papers in which they are photographically illustrated.
Shape: P = plan; V = vertical cross-section. The inferred depositional settings noted are those provided in the publication cited. Molar tooth structures and septarian cracks are not included.
CO_3, carbonate present as a cement; Fm, Formation; Mb, Member; MISS, putative microbially-induced sedimentary structures in close stratigraphic proximity to cracks; ND, not determined.

through the Phanerozoic. Most are found in heterolithic facies, in which mudstone-hosted cracks are filled with sand or silt sourced from the adjacent beds. There are also numerous examples of cracks in sandstones, particularly along ripple-troughs. The host rock may be totally free of clay (e.g. Fairchild 1980; Pflueger 1999; Gehling 2000) and, in many instances, is either composed of, or cemented by, carbonate. Cracks are sometimes filled with sparry calcite or dolomite.

In plan view, subaqueous sedimentary cracks are typically spindle-shaped and form incomplete polygons; there is a continuum from isolated aligned or non-aligned spindles through to branching/bifurcating spindles (including 'bird's foot' triple junctions), partial polygons and complete polygons (Fig. 1a–d). The morphology is seldom adequate to confirm a subaqueous mode of origin (Tanner 2003). Although most subaqueous cracks are straight-sided or gently curved, some examples, known as curlicue cracks, are curved to an extent that is atypical of desiccation cracks (e.g. Cowan & James 1992; Patel *et al.* 2013; Fig. 1e). Sinuous cracks occurring in wave ripple-troughs are known as Manchuriophycus and occur in numerous pre-Mesozoic sandstones and at least one Proterozoic carbonate (Xiaoying *et al.* 2008). Manchuriophycus cracks are always confined within a single ripple-trough and oriented parallel to it (Fig. 1f), but may curve sharply, describe figures of eight or branch. The Latinate name *Manchuriophycus* was assigned to these structures when they were thought to be trace fossils. Now that they are known to be pseudofossils, the name is retained, but should not be italicized.

Subaqueous sedimentary cracks are generally vertical or subvertical in orientation, may cut multiple thin beds, taper upwards or downwards, or both, and are often spindle-shaped in vertical cross-sections (e.g. Kidder 1990; Cowan & James 1992; Hughes & Hesselbo 1997; Pratt 1998*a*; Bhattacharya & MacEachern 2009). Many examples bifurcate either upwards or downwards (e.g. Kidder 1990; Harazim *et al.* 2013; Fig. 1g). The infill is commonly contiguous with an overlying or underlying bed, and sometimes both. Cracks in thick mudstones are typically sinuously or ptygmatically folded in the vertical plane, presumably because the crack-fill was more resistant to burial compaction than the matrix. For the same reason, the presence of filled cracks often limits the compaction of adjacent sediment, producing a local, tent-like thickening of the host bed (Fig. 1h).

Cracks in bedded carbonate facies

Diverse carbonate facies host crack-like structures (Figs 2 & 3) that may be, in some ways, analogous to those occurring in purely siliciclastic rocks. In

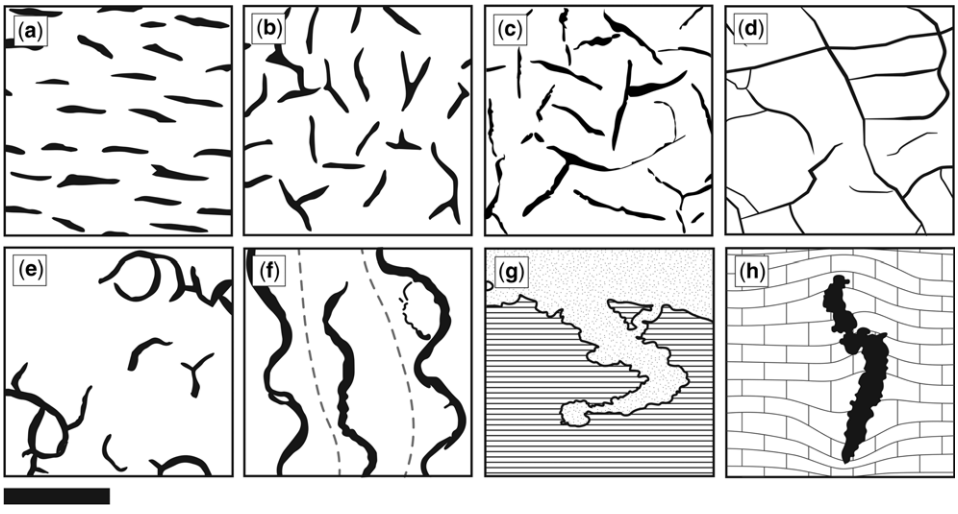

Fig. 1. Typical crack morphologies expressed on bedding planes (a–f) and in vertical cross-section (g, h). (**a**) Isolated aligned spindles (Donovan & Foster 1972). (**b**) Branching spindles and triple-junction bird's feet (Donovan & Foster 1972). (**c**) Partially connected branches (after Pflueger 1999). (**d**) Connected branches and polygons (Tanner 1998). (**e**) Curlicue cracks (Patel *et al*. 2013). (**f**) Sinuous ripple-trough cracks; ripple crests dashed (after Pflueger 1999). (**g**) Vertical cross-section of downwards-tapering, upwards-bifurcating, ptygmatically folded sand-filled crack in mudstone (after Harazim *et al.* 2013). (**h**) Vertical cross-section of upwards- and downwards-tapering, ptygmatically folded microspar-filled crack (molar tooth) in limestone showing distortion of background laminae (after Fairchild & Hambrey 1984). Scale bars: a–f, 50 mm; g, 7 mm; h, 15 mm.

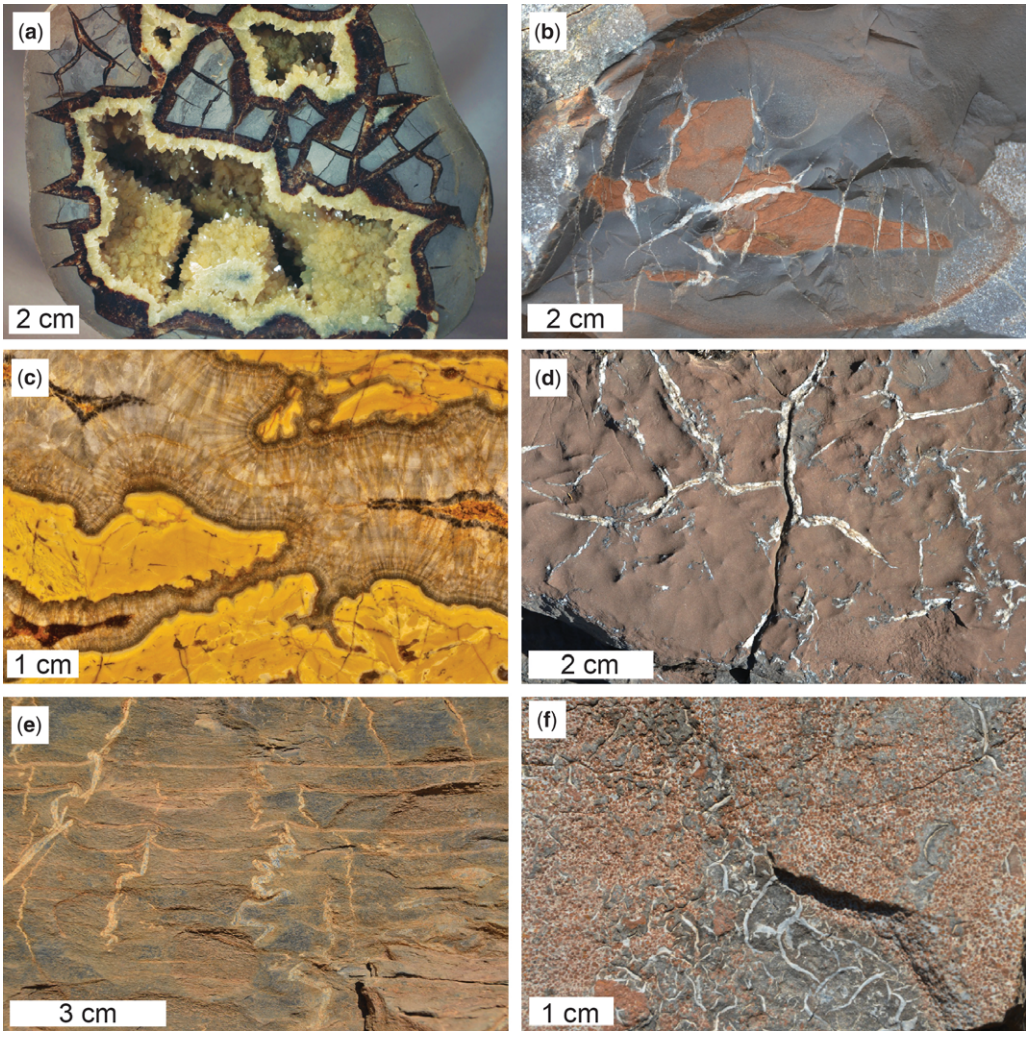

Fig. 2. Photographs of subaqueous sedimentary cracks in carbonates. (**a**) Cut and polished septarian concretion in Cretaceous limestone of Cretaceous age (Utah; stratigraphy unrecorded) showing brown aragonite cementing cracks and yellow calcite lining interior cavities. (**b**) *In situ* septarian concretion in the Neoarchaean Griquatown Iron Formation of South Africa (dolomitized and partially silicified), which may have formed from shrinkage during carbonate nodule growth (prior to silicification) or may have formed from the shrinkage of a silica gel during chert formation (Beukes 1984). (**c**) Cut and polished sheet cavities from the shallow back-reef facies of the Cryogenian Balcanoona Formation, South Australia, with fibrous isopachous marine cement. (**d**) Plan view of a carbonate bedding surface from the Neoarchaean Gamohaan Formation (South Africa) showing subaqueously formed molar tooth cracks. (**e**, **f**) Vertical cross-section and plan view (respectively) of molar tooth cracks in calcareous shale beds in the Neoarchaean Monteville Formation (South Africa) showing ptygmatic vertical cross-sections and a curved, branching morphology in plan view.

addition to forms similar to cracks in siliciclastic facies, carbonates host radiating septarian cracks in nodules (Fig. 2a, b), sheet cavities (or sheet cracks) (Figs 2c & 3a) and molar tooth structures (MTS; Figs 2d–f & 3b, Table 1). These structures, which vary broadly in morphology and infill, are most common in Precambrian to early Palaeozoic carbonates, but, with the exception of MTS, are also found throughout the Phanerozoic. Subaqueous sedimentary and very early diagenetic cracks in carbonate facies are usually centimetre-scale and sharp-walled, and are filled by either calcite spar, clay or carbonate sediment. These structures display a similar array of morphologies to those in

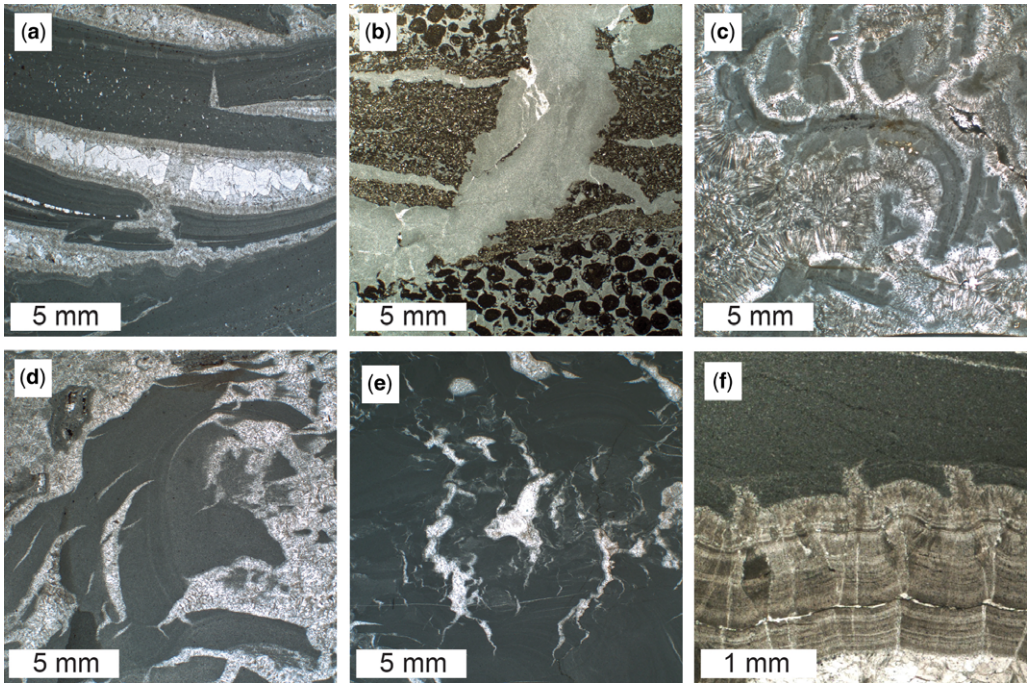

Fig. 3. Photomicrographs of subaqueous carbonate sedimentary cracks in vertical cross-section. (**a**) Sheet cavities from shallow platform facies of the *c.* 650 Ma Gauss Formation, Namibia. (**b**) Molar tooth cracks from the Monteville Formation, South Africa (*c.* 2.6 Ga). These ptygmatic to linear cracks occur in swarms in finer carbonate–clay beds of the formation and are filled with very finely crystalline calcite spar. (**c**) Cryogenian (*c.* 650 Ma) platform reefal dolomites of the Balcanoona Formation, South Australia. Micritic dolomites have cracked along layers and curled up to form mud chips, which have cracked further and been cemented by marine cements. (**d**, **e**) Ptygmatic and linear cracks from shallow platform facies of the *c.* 650 Ma Gauss Formation, Namibia. (**f**) Subaqueous cracks from the *c.* 760 Ma Devede Formation, Namibia, which are interpreted to have formed by subaqueous dehydration of carbonate precursor minerals during dolomitization and dolomite marine cement precipitation (Hood *et al.* 2015).

purely siliciclastic sediments, including ptygmatic, linear, curved and spindle-shaped vertical cross-sections. Cracks may be multigenerational and commonly initiate at bedding planes, but may also occur within beds.

Subaqueous cracks are found in diverse carbonate lithologies, including pure limestones and dolomites, as well as argillaceous carbonates deposited in shallow marine to slope settings. Cracks in the latter settings are morphologically similar to cracks described from purely siliciclastic sequences (e.g. Donovan & Foster 1972). Some cracks are particularly well developed at carbonate–mudstone interfaces in heterolithic facies. The associated carbonates can be relatively coarse grainstones (e.g. Cowan & James 1992). Cracks in these settings are typically centimetre-scale, most commonly vertical and exhibit either a tapered V-shaped or U-shaped linear morphology or an open anastomosing shape, which is often spindle or cuspate in vertical cross-section. On upper bed surfaces, cracks may form polygonal networks, isolated linear cracks or curlicue cracks. The infill of the cracks is commonly either micritic sediment (with minor clay) from surrounding beds, which may form geopetal surfaces, or clear calcite spar without sediment.

Carbonates with a low clay content may also contain subaqueous synsedimentary cracks, which are especially prevalent in intertidal to shallow marine platform settings, where cracking can be pervasive (Table 1). A range of lithologies – including ooid and peloid grainstones, micritic carbonates and sediments associated with microbial structures – may host cracks. Cracks in carbonates may be curved, ptygmatic or linear in vertical cross-section and are commonly filled by either fibrous or sparry isopachous cements of dolomitic or calcitic composition (e.g. Hood *et al.* 2015; our Figs 2c & 3a–f). Cracks may also be silicified. They can develop in the vertical plane, but are commonly affected by the geometry of depositional laminations. Well-developed cracked lithologies show

more irregular, bulbous, sinuous and dendritic crack patterns. In some cases, intense cracking is associated with brecciation of the substrate, whereby some beds are disrupted to form intraclasts that are themselves often cracked and curled (Harwood & Sumner 2011 (only subaqueous in some facies); Hood *et al.* 2015). In many cases, cracked carbonate substrates are associated with microbialites or stromatolites and may preferentially form in microbialitic layers or in reworked intraclasts of microbial sediment. Examples of cracked carbonates are most common in the Precambrian, possibly because of oceanic carbonate supersaturation and the lack of bioturbation (Frank & Lyons 1998; Hood *et al.* 2015). Cracking of this type has been attributed to evaporite solution–collapse–brecciation (e.g. Pomoni-Papaioannou & Karakitsios 2002), the subaqueous dehydration of hydrous carbonate minerals (Hood *et al.* 2015), synaeresis (Fairchild 1980) and diastasis (Cowan & James 1992; see later in this paper).

Field observations of Precambrian carbonates from Australia and Namibia indicate that cracked lithologies are commonly marine-cemented (e.g. Hoffman & Macdonald 2010; Hood *et al.* 2015; our Fig. 2c). Although early carbonate precipitation has been inferred to inhibit crack formation in fine-grained clastic rocks, it may be essential to their preservation through burial compaction (Calver & Baillie 1990).

Septarian cracks

Septarian cracks in carbonate nodules are a form of early diagenetic shrinkage crack typically associated with concretion formation, just under the sediment–water interface (Astin 1986; Duck 1995). These cracks are present within nodular and cylindrical carbonate concretions that are progressively cemented outwards, forming broadly radial cracks that are widest at the nodule centre and taper towards the outer margin of the concretion (Fig. 2a, b; Raiswell 1971; Astin 1986). Septarian cracks are generally polygonal in bedding-parallel sections, fairly straight and approximately perpendicular to bedding in vertical cross-section. Several generations of crack may be present within a single nodule. Septarian cracks have also been observed in chert nodules from marine and lacustrine Precambrian to modern sediments (Beukes 1984; Schubel & Simonson 1990).

Molar tooth structures

The enigmatic MTS are considered to represent subaqueous, carbonate-filled cavities in carbonate rocks, the origin of which remains contentious (e.g. Furniss *et al.* 1998; James *et al.* 1998; Shields 2002; Bishop *et al.* 2006; Shen *et al.* 2016; our Fig. 2d–f). MTS can be distinguished primarily by their infill, which consists of rapidly lithified, microcrystalline blocky calcite (Shields 2002), and typically form long, vertically oriented ribbon-like cracks, which may be sinuously or ptygmatically folded with burial compaction. They are hosted in dolomites, limestones and argillaceous carbonates and are generally found in shallow platform marine facies. There is disagreement about whether MTS should really be considered as cracks or voids, which hinges on the choice of genetic interpretation (Pratt 1998*b*; Winston *et al.* 1999). However, many MTS are similar to other subaqueous sedimentary cracks in their mineralogy and morphology. Cracks may be several centimetres long and have discrete margins (Fig. 3b). They are infilled by clear, finely crystalline 5–15 μm equant calcite spar crystals, only rarely containing internal sediment (James *et al.* 1998; Bishop *et al.* 2006). The calcite microspar infill may be deformed within the sediments prior to lithification. It may also be eroded, broken and redeposited as intraclasts by high-energy currents while only partially lithified, suggesting a syn-sedimentary origin for these structures. They are most common in late Archaean to Neoproterozoic sediments (Shields 2002). Microspar-filled cracks have also been described from Archaean calcareous shales (Bishop *et al.* 2006) and calcareous siliciclastic rocks (e.g. Calver & Baillie 1990; Turner *et al.* 1997), suggesting that these structures are not limited to pure carbonate settings. For a more specific literature review of MTS and their occurrence, see Kuang 2014.

Sheet cavities

Sheet cavities, or sheet cracks, are bedding-parallel sedimentary fractures in carbonates, often associated with tepee structures in shallow marine settings (Figs 2c & 3a). Similar structures may also form in more intertidal to peritidal settings (e.g. the Cryogenian Angepena Formation, Giddings *et al.* 2009; Hood & Wallace 2012), but are less well developed and may be associated with sub-aerial exposure. These cavities form bedding-parallel laminoid networks that may be planar or buckled and are occasionally connected between beds. The filled cracks may be several centimetres in height (generally <10 cm) and up to 2 m across and are lined with isopachous, fibrous carbonate cements that occasionally overlie pendant and laminated micritic microbial fills. These features are more common in Precambrian platform carbonates (e.g. Jiang *et al.* 2006; Giddings *et al.* 2009; Hoffman & Macdonald 2010; Hood & Wallace 2012), but also occur in Phanerozoic carbonate platforms (e.g. Assereto & Kendall 1977). These bedded, cracked

and cemented structures, associated with tepees and often fenestrae, resemble the shallow, subaqueous Holocene hardgrounds of Shinn (1969) in their buckled, bedding-parallel morphology and association with early cementation.

Case study: Hales Limestone, Tybo Canyon, Nevada

The carbonate slope succession in the Cambro-Ordovician Hales Limestone of Tybo Canyon, Nevada contains argillaceous carbonates with sedimentary cracks (Cook & Taylor 1977; Marek 2015; our Fig. 4). This unit consists of interbedded carbonates and shales between 5 cm and 1 m in thickness, which may be slumped and include carbonate intraclast debrites. Cracks are typically found within carbonate beds, often at the interface with overlying shale, and may also be present in carbonate nodules higher in the section. Cracks are generally vertically oriented, V-shaped, several centimetres in height and only a few millimetres wide. The crack morphology is linear or sharply zigzagging in vertical cross-section, particularly in smaller examples, but may be ptygmatically contorted in larger cracks (Fig. 4a, b). Cracks may form polygonal networks or isolated bird's foot shapes on bedding planes (Fig. 4c, d). Cracks are filled with coarse, clear calcite spar, but may also be filled with a mix of carbonate micrite and argillaceous sediment. Anastomosing cracks are partially filled by geopetal sediment, which accumulated on horizontally cracked sections beneath a sparry calcite-fill. The coarseness of this calcite spar infill, and the geopetal nature of the internal sediment, distinguishes these cracks from MTS. The presence of this geopetal infill suggests that the cracks were open near or at the sediment–water interface, allowing sediment to accumulate within the cracks. Some cracks are draped by argillaceous–micritic laminae

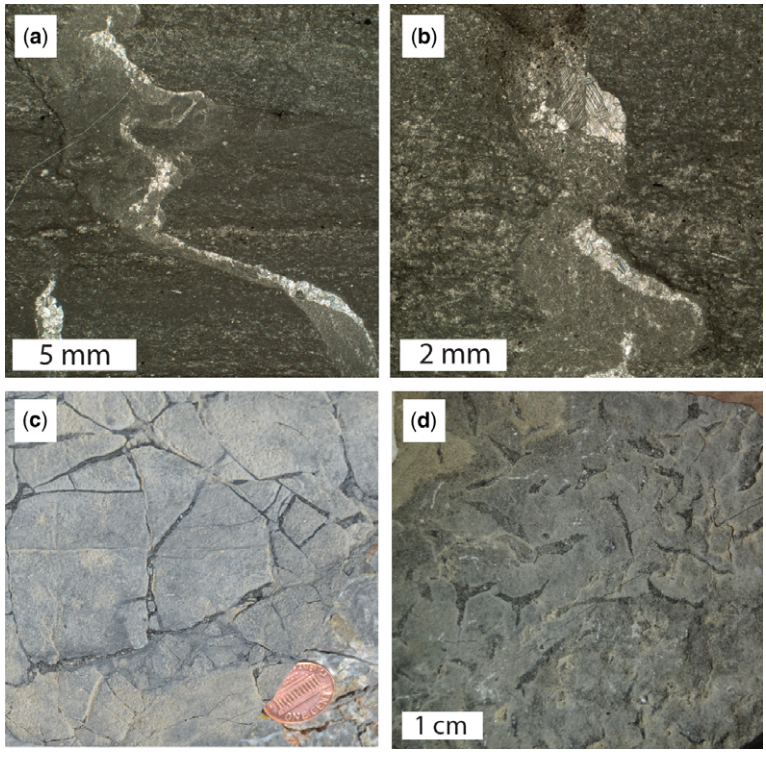

Fig. 4. Late Ordovician–Early Cambrian examples of subaqueous sedimentary cracks from the slope facies of the Hales Limestone of Tybo Canyon, Nevada. (**a**, **b**) Thin section photomicrographs of curved to ptygmatic cracks in fine-grained turbidites and debris flow beds. Cracks have filled with calcite micrite and clay, forming geopetal surfaces and have subsequently been filled with clear calcite spar. In (b), sediment from the overlying bed forms part of the geopetal infill near the top of the sedimentary crack. (**c**) Outcrop photo or bedding surface of cracked carbonate beds in the Hales Limestone, showing generally linear, branching morphology in plan view, resembling joints. (**d**) Outcrop photo of cracks on a bedding plane showing bird's foot triple-junction morphology (cf. Donovan & Foster 1972).

from the overlying bed on their upper surfaces (e.g. Fig. 4b). Particulate matter from the draped material is cemented in place by the coarse calcite spar crack-fill. This could indicate that the limestone beds were stabilized prior to the next bed of sediment being deposited (perhaps by a biofilm), allowing the sediment to drape over the open crack. Alternatively, it is possible that initial calcite cementation was early enough to stabilize and entrain particulate matter from the overlying sediment.

Origin of subaqueous cracks: geological evidence

Sedimentary cracking in general can be regarded as a two-part process: (1) the sediment must acquire the intergranular adhesion necessary to crack rather than flow or deform; and (2) some stress must be applied to initiate the cracking itself. In the formation of desiccation cracks, cohesion is provided by the surface tension of the films of water enveloping the grains, while differential dehydration within the sediment generates the necessary stress field. However, in principle, the processes stiffening and subsequently cracking sediments could be completely independent (e.g. Harazim *et al.* 2013).

Most researchers have inferred that subaqueous cracking occurs at or near the sediment–water interface through the de-watering of recently deposited argillaceous sediment. The concomitant volume change causes the opening of cracks that are then either passively filled by other sediments or lost to compaction, mixing and erosion. There is, however, little, if any, field evidence to indicate that such processes operate in modern sediments. In recent years, several researchers have suggested that cracks form well below the sediment–water interface, where preservation in the geological record is more likely and observation in modern sediments is less straightforward (Tanner 2003; Harazim *et al.* 2013). Although many cracks taper downwards like desiccation cracks, others taper at both the top and bottom along most of their lengths, which suggests a truly intrastratal origin, but may also result from bulging of the crack-fill during compaction (Cowan & James 1992; Pratt 1998*a*). In at least one instance, cracks filled from above are clearly the focus of subsidence in the overlying layer, which must therefore have been deposited before the cracks opened (Hughes & Hesselbo 1997). Cracks can also occur at the base of a mudstone bed and taper upwards, implying sand injection from below (Pratt 1998*a*, *b*).

The explanations previously proposed for subaqueous crack formation can be grouped into five main families: (1) salinity-related synaeresis; (2) loading or compaction; (3) seismic activity; (4) microbial processes; and (5) authigenic mineralization. We evaluate these in the light of the existing geological evidence, before proceeding to discuss existing experimental results, including our own.

Salinity-related synaeresis

Synaeresis (or syneresis) – the ejection of water from contracting gels – is a widespread physical process first mentioned in connection with sedimentary cracks by Jüngst (1934). The term has since been used to describe (and sometimes confound) two different processes occurring in clays – namely, deflocculation and intracrystalline de-watering. Deflocculation occurs because suspended clay particles in saline water are mutually attractive, assembling spontaneously into fluffy flocs in which randomly oriented grains loosely pack together, allowing for considerable de-watering and reduction in volume when the grains are reoriented in the first stages of burial and compaction. Intracrystalline de-watering, in contrast, depends on the crystallographic structure of swelling clays (smectites), which absorb and release water osmotically within interlayer spaces. It has been suggested that deflocculation causes sufficient shrinkage to open tensile cracks near the sediment–water interface (White 1961). As increasing the salinity decreases the water-retention capacity of subaqueous swelling clays, it has also been inferred that intracrystalline de-watering could open cracks at and near the sediment–water interface in smectitic muds when the ambient salinity is increased (by, for example, an influx of seawater into a brackish lagoon or tidal channel; Burst 1965).

The occurrence of subaqueous sedimentary cracks in marine rocks is commonly taken to indicate fluctuating palaeosalinity stress (e.g. Carroll & Wartes 2003; Bhattacharya & MacEachern 2009; Buatois *et al.* 2011). However, geological evidence shows that this inference cannot be valid in all cases (Tanner 2003; Harazim *et al.* 2013). Subaqueous cracks occur in clay-free carbonates and sandstones (e.g. Fairchild 1980; Pflueger 1999; Gehling 2000) and are not limited to marginal sediments, but occur in marine, brackish and lacustrine facies representing a wide range of palaeosalinities (Pratt 1998*a*). Most examples are not associated with evidence of salinity stress (Harazim *et al.* 2013). Sedimentologists have long sought a palaeoenvironmental proxy for fluctuating salinity, especially since the recognition of estuarine deposits in incised valley-fills has become a crucial part of sequence stratigraphic analysis (Zaitlin *et al.* 1994). In the absence of unambiguous alternatives, low ichnological diversity and synaeresis cracks have been widely used. Subaqueous cracks do commonly occur in mudstones without significant bioturbation

and with low ichnological diversity, but inferring that low ichnological diversity is due to salinity stress underestimates the importance of mud fluidity and hypoxia in the same marginal marine settings (McIlroy 2004). Many physicochemical properties (e.g. a limited availability of organic matter) and biological processes are common to depositional settings that are stressful to burrowing organisms. As such, the inference that synaeresis cracks must result from salinity fluctuation because they occur in minimally bioturbated facies is misguided.

Subaqueous cracking induced by loading, burial or wave-induced stress

Compaction during burial may both de-water mud (stiffening and shrinking it) and initiate cracking by purely mechanical means; the vertical to subvertical orientation of most cracks may be an expression of lateral tension resulting from vertical compression (White 1961; Plummer & Gostin 1981; Kidder 1990). However, if ordinary compaction alone were sufficient to generate subaqueous cracks, they should be much more common than they are (Tanner 1998). If there is an additional factor contributing to crack formation (and preservation) under compression, it may lie either in the extremity of the applied stress, the stiffness of the substrate or the superposition of the stiffened substrate over a highly compressible layer (e.g. a microbial mat over sediment rich in porewater; Harazim *et al.* 2013). Instead of cracking, an insufficiently stiff mud would produce soft sediment deformation structures and potentially undergo density inversion on the rapid introduction of a heavy sand load (Harazim *et al.* 2013).

In addition to rapid sediment loading, it has been inferred that hydraulic pressure arising from the passage of sea waves may generate shear and tensile stresses near the sediment–water interface, causing the mechanical failure of stiff mud layers without shrinking or de-watering (Cowan & James 1992). This model applies equally to fine-grained siliciclastic and carbonate sediments, but is neutral about the mechanism by which the stiffening of mud occurs. The phenomenon has been termed diastasis and is inferred to generate diastasis cracks. Diastasis cracks are fracture networks first described from the interbedded muddy and allochemical carbonates of the Late Cambrian Port au Port Group of Newfoundland, Canada (Cowan & James 1992). In plan view, these fractures form polygonal networks, sub-parallel spindles and curlicues. In vertical cross-section, they reveal features that clearly demonstrate brittle cracking with minimal, if any, associated volume change. The cracks have either straight or jagged walls and they bifurcate and ramify to cause complete brecciation with rip-up clasts. Many of the cracks are hairline fractures. Some are partially dilated by compression and/or lateral tension, whereas others remain closed. Most of the cracks illustrated by Cowan & James (1992) completely bisected the mudstone beds in which they were found and several of them resembled miniature normal faults. These examples are compelling, but unusual.

If cracking were primarily induced by sediment loading at or near the sediment–water interface, a spectrum from sharp cracks to load casts would be expected because sediment stiffness is a matter of degree. One possible candidate for an intermediate structure, consisting of a network of irregular, roughly quadrilateral sand-filled 'cracks' attached to and associated with ball-and-pillow load structures, is found in the Neoproterozoic Ediacara Member (Rawnsley Quartzite) of South Australia's Flinders Ranges (Gehling 2000). A similar array of rectilinear, downwards-tapering, V-shaped, bulging sand-filled cracks was reported from Silurian rocks in the Murzuk Basin of Libya by Pflueger (1999), who described it as a network of load cracks. Although distinguished by their rectangular patterning, these structures might be related to polygonal density inversion structures (Anketell *et al.* 1970; Morrow 1972). Elsewhere in the Flinders Ranges, unambiguous cracks in the Brachina Formation and the overlying ABC Range Formation are associated with load structures where sandstone and siltstone beds overlie shales (Plummer & Gostin 1981). A similar association has been reported in the Triassic Arroyo Malo Formation of South America (Lanés *et al.* 2008). Cracks have also been reported from other successions in mudstones immediately underlying sands deposited from storms or other intense hydrodynamic events (e.g. Kidder 1990; Harazim *et al.* 2013). This evidence should be treated with caution because it may partly result from a preservational bias: mud-hosted cracks are much more likely to be preserved and recognized in the rock record if they are filled with sand and, in many heterolithic successions, sand is only deposited in high-energy events. In addition, many instances of subaqueous sedimentary cracks can be adduced from low energy, low sedimentation rate palaeoenvironments (e.g. Calver & Baillie 1990; Carroll & Wartes 2003; Timms *et al.* 2015).

Seismically induced cracking

Some researchers have suggested that the majority of subaqueous sedimentary cracks in the geological record are the result of earthquakes (Pratt 1998*a*), a conclusion that has been extrapolated to include mechanisms for the formation of MTS (Pratt 1998*b*) and cracks in septarian concretions (Pratt

2001). This work is based on the precept that seismic shaking causes randomly oriented clay particles in mud to collapse into the horizontal plane, thereby expelling porewater and opening fissures into which liquefied sand is injected from adjacent layers. (Pratt 1998*a*; Tanner 1998). Fairchild *et al.* (1997) instead emphasized the potential for seismic waves to mechanically fracture stiff subaqueous sediments.

Pratt (1998*a*) listed 15 features of subaqueous sedimentary cracks that he found to be suggestive of a seismic mode of origin. Most compellingly, Pratt stated that cracks are more common in rift basins than on passive margins. Whether or not this is the case, many examples of cracks can be adduced from basins that were probably tectonically stable at the relevant time (e.g. Hughes & Hesselbo 1997; Chen *et al.* 2009; Harazim *et al.* 2013). On the other hand, we agree with Shields (2002) that the remarkable lateral extent of MTS in the Taoudeni Basin of NW Africa, measured as hundreds of kilometres, is most parsimoniously explained by a tectonic control on their formation.

Pratt (1998*a*) observed that cracking and associated sand injection appear to have occurred in all directions (including upwards), sometimes simultaneously, which he took to imply isotropic contraction inconsistent with a vertical hydraulic gradient being the cause of shrinkage. Against this view, we note that the vast majority of cracks are approximately vertical and are filled, not from below, but from above (Harazim *et al.* 2013). This suggests that crack-filling is predominantly geopetal and only occasionally a consequence of sand injection; subaqueous crack patterns are thus clearly distinct from the sand dykelet swarms commonly associated with palaeoseismicity (e.g. Winslow 1983). Pratt (1998*a*) also remarked that some sandstones and siltstones intercalated with crack-bearing mudstone beds showed evidence of churning or folding due to liquefaction. Fairchild *et al.* (1997) and Shields (2002) likewise noted an association between liquefaction features and MTS and accordingly favoured a seismic mode of origin (e.g. Fairchild *et al.* 1997; Shields 2002). However, such features are far from ubiquitous and liquefaction (and injection) can result from static overpressure as well as seismic shock.

Microbial processes

In recent decades, a number of researchers have sought to relate the formation of subaqueous cracks to the activity of microorganisms in sediment (e.g. Furniss *et al.* 1998; Gehling 1999; Harazim *et al.* 2013; Shen *et al.* 2016). Microbes could, in principle, contribute to both parts of the process of sedimentary cracking, i.e. the development of intergranular adhesion and the disruption of the cohesive sediment. It is well established that microbes and their extracellular polymeric substances stabilize organic-rich sediments and that microbial gas bubbles may simultaneously produce void space and stiffen the surrounding sediment by entraining and removing water (Furniss *et al.* 1998). Harazim *et al.* (2013) have suggested that the decay of buried microbial mats may promote the formation of such voids in some settings. They have also suggested that biostabilization by microbial mats at the sediment–water interface might restrict the movement of the underlying porewater-rich mud so that post-burial shrinkage can only be accommodated by cracking. In organic-rich muds in the Baltic Sea, interconnected voids full of microbial methane gas have been X-rayed *in situ* tens of centimetres below the sediment–water interface; these voids resemble sedimentary cracks in shape, size and orientation (Abegg & Anderson 1997). Although unfilled, these microbial gas voids are a promising analogue for ancient subaqueous sedimentary cracks (Furniss *et al.* 1998).

The clearest geological evidence for a microbial role in subaqueous cracking in siliciclastic facies is provided by sinuous ripple-trough and branching spindle cracks in pure sandstones, the grains of which would have accommodated stress by moving past one another rather than opening cracks unless they were bound together by biofilms. Good examples are found in the Ediacara Member of the Rawnsley Quartzite (Australia; Gehling 2000) and the Acacus Formation in the Silurian of Libya (Pflueger 1999). Harazim *et al.* (2013) have found additional evidence for microbially-induced cracking in an Ordovician mudstone. They reported a shift towards lighter carbon isotope compositions associated with an increase in organic matter content towards the upper surface of an intrastratally cracked bed in the heterolithic Beach Formation of Newfoundland. In thin section, these beds display crinkly laminations typical of microbial mats. Mudstone cracks have rarely been investigated in this way, so it is not yet clear how representative these results may be. However, it is clear that some subaqueous sedimentary cracks occur without any associated microbially-induced sedimentary structures (MISS; Table 1). More tellingly, cracks have been found in well-bioturbated mudstones and even directly associated with large burrows, precluding a role for well-developed microbial mats in these instances (Davies *et al.* 2016). Such pervasive bioturbation dramatically impedes the normal biostabilization of sediment as well as the development of microbial mats (De Deckere *et al.* 2001).

A microbial contribution to the formation of MTS has been widely discussed, primarily because many of them resemble gas bubbles or gas escape tunnels in their morphology (described as ribbon

and blob morphology; Furniss *et al.* 1998). Carbon isotopes indicate that molar tooth calcite was not derived from biogenic methane, but such a gas might still have opened the cracks prior to the rapid precipitation of porewater-derived carbonate (Frank & Lyons 1998; Shen *et al.* 2016). Sulphur isotopic evidence suggests that MTS formed in the sulphidic zone in the sediment column, where high alkalinity induced by bacterial sulphate reduction favoured rapid carbonate precipitation (Shen *et al.* 2016). Similarly, sheet cracks, synsedimentary breccias and cavities in the Doushantuo Formation cap carbonate (*c.* 635 Ma) are cemented by carbonate bearing the isotopic signature of microbial methane oxidation (as well as pyrite and barite suggestive of microbial sulphur cycling), but the structures themselves are most likely to be a product of methane seepage (Jiang *et al.* 2006).

Authigenic mineralization

Authigenic mineralization/cementation in sediments and synsedimentary diagenetic phase changes in minerals are underrepresented as possible mechanisms in the literature on subaqueous crack formation. Siliciclastic horizons hosting cracks are commonly carbonate-cemented (Table 1) and incipient carbonate cementation has been inferred to explain the stiffening observed in modern marine muds a few decimetres below the sediment–water interface (Fairchild *et al.* 1997). Early carbonate cementation may have stiffened sediments in a wide range of facies and thereby facilitated subsequent cracking (Jüngst 1934; Fairchild *et al.* 1997; Chen *et al.* 2009; Hood *et al.* 2015). It is widely recognized that carbonate cementation can cause sediment expansion, buckling and cracking in shallow marine carbonates (e.g. hardgrounds, Shinn 1969; curl breccias, Hood *et al.* 2015). Heterogeneous or differential early carbonate cementation of a sediment pile has also been implicated in sediment cracking and brecciation in interbedded clastic and carbonate lithologies (Chen *et al.* 2009).

Calcareous sediments are susceptible to recrystallization during sedimentation and early diagenesis. The dehydration of an amorphous calcium carbonate precursor with the formation of more stable carbonate minerals has been emphasized in many different forms of carbonate precipitation (Rodriguez-Blanco *et al.* 2011, 2014). Such phase changes, specifically the subaqueous dehydration of hydrous, amorphous minerals and the associated volume changes of precipitates, have been implicated in the sedimentary cracking of Precambrian carbonates, forming cracked beds, intraclasts and sheet cavities (e.g. Hood *et al.* 2015). High $CaCO_3$ supersaturation during much of the Precambrian may have further promoted the rapid and widespread precipitation of authigenic amorphous carbonate minerals such as these, perhaps going some way to explain the abundance of these features preserved in the Proterozoic rock record (Shields 2002; Higgins *et al.* 2009).

Other forms of sedimentary cracking have also been suggested to be a result of phase changes, including crystallographic dehydration or authigenic mineral replacement during synsedimentary diagenesis. Although septarian cracking has been suggested to occur via several mechanisms, including earthquake-induced cracking (Pratt 2001) and tensile fracturing during compaction (Astin 1986), it has also been proposed to be induced by subaqueous shrinkage and density changes from the conversion of the initial calcium precipitates (related to the decay of organic matter) to calcium carbonate (Duck 1995). Similarly, septarian cracks in cherts are thought to form during the transformation of a precursor hydrous mineral (magadiite or similar) to quartz during silicification during early diagenesis (Schubel & Simonson 1990). Archaean marine chert nodules have also been proposed to form from the shrinkage of a silica gel during chert formation (Beukes 1984). MTS are also suggested to have formed in substrates under oceans highly supersaturated with respect to carbonate, rapidly precipitating and cementing carbonate lithologies (Frank & Lyons 1998; Shields 2002). The microspar infill of these cracks, whether cement or crystal silt, is rapidly lithified, allowing it to be reworked as intraclasts during sedimentation, suggesting that rapid carbonate cementation is an important process in the preservation, and perhaps formation, of these structures. It has been proposed that MTS formed by the replacement of a precursor biotic component (Smith 1968) or evaporite mineral (Eby 1977), although a lack of evaporite pseudomorphs and the presence of sharp contacts at the margins of these cracks argue against these hypotheses (e.g. Frank & Lyons 1998).

Previous experimental evidence

Jüngst (1934) found that pits, cones, mounds and cracks similar to those seen in ancient mudstones can be produced in the laboratory by allowing natural colloidal sediments to settle out of suspension. He found that dissolved salts enhance, but are not necessary for, crack formation, which is consistent with synaeretic de-watering. His classic paper describes (but unfortunately does not illustrate) the subaqueous development of polygonal cracks in fast-hardening muds (especially calcareous or sandy clay mixtures). These cracks were reportedly up to 3 cm deep and 3 mm wide and resembled the cracks seen in calcareous marls in the Middle Triassic of Germany (Jüngst 1934). In subsequent

experimental work by White (1961), a saline clay slurry was poured onto a filter, where the clay flocculated and settled leaving water on top (the composition of the clay was not recorded). The filter cake quickly developed small, randomly oriented cracks. If the clay minerals were suspended in distilled rather than saline water, they dispersed instead of flocculating and settled into a more compact, laminated filter cake that did not develop cracks. The effect of increasing salinity was investigated by Burst (1965), who performed an experiment in which bentonite mixed with distilled water was placed on a filter. Distilled water lost through the filter was continually replenished with salt water so that the slurry became increasingly saline without drying out. Long, curving, vertical cracks developed in the upper surface of the filter cake after two weeks. Pure kaolinite and other non-swelling clays could not be induced to crack in this way, but mixtures containing only 2% bentonite cracked and higher fractions of bentonite were associated with more abundant and penetrative cracks (Burst 1965). Burst (1965), unfortunately, did not conduct control experiments holding the salinity constant. Experimentally produced synaeresis cracks have so far been limited to small, straight or curved spindles and polygons in clays. They have not been demonstrated to entrain sand from above or below, or to develop in clay-free carbonate colloids, as proposed by Fairchild (1980). There is therefore considerable scope for more sophisticated experimental work to be carried out.

Many workers have experimentally investigated the deformation of sediments by loading and compaction, but few, if any, of the resulting structures have convincingly resembled sedimentary cracks. The laboratory deformation of soft, subaqueous heterolithic sediment of different densities has generated polygonal patterns of upwards and downward sand penetration into adjacent mud (Anketell *et al.* 1970), but the structures produced were globular and not tapering in their extremities and thus unlike subaqueous sedimentary cracks. The same researchers briefly described the formation of V-shaped cracks in brittle layers enclosed between plastic mud layers when mechanical forces were applied (Anketell *et al.* 1970), but did not provide an illustration. Mörz *et al.* (2013) generated an array of interesting branching fluid escape structures by applying hydraulic pressure to the base of a sediment pile. Some of these structures resembled sedimentary cracks in vertical cross-section, but they were broadly cylindrical rather than planar in morphology (cf. Menon *et al.* 2016).

There is currently no experimental evidence that seismic shaking, authigenic mineralization or early diagenetic phase changes can induce subaqueous cracking (earthquake simulations have produced soft sediment deformation structures, but they do not resemble subaqueous cracks; e.g. Owen 1996). Models involving microbial processes have only been tested in the case of MTS. Furniss *et al.* (1998) were able to produce voids resembling the blob and sheet pattern of MTS using yeast cultures incubated with sugar in mixtures of clay and plaster of Paris. The respiring yeast rapidly produced bubbles of carbon dioxide. Sealing of the sediment surface was necessary to force the bubbles of carbon dioxide to shoot through the mixture, leaving the voids behind.

New experimental evidence

We carried out 26 laboratory experiments to investigate subaqueous crack formation in sediments. The experimental conditions are summarized in Table 2.

Materials

The sediment types and layering configurations are shown in Figure 5. The sediments used were: (1) sodium montmorillonite (Wyoming, USA; Clay Minerals Society; Fig. 5a) washed in deionized water, sonicated and centrifuged at 1000 rpm for five minutes to accelerate deposition; (2) silty estuarine mud collected from Long Wharf, New Haven, Connecticut, USA (41.2941° N, 72.9170° W), sterilized in an autoclave (interlayered with sand in Fig. 5b); (c) calcium montmorillonite (Gonzales County, Texas, USA; Clay Minerals Society; washed in deionized water; interlayered with sand in Fig. 5c); (4) the same calcium montmorillonite, mixed 3:1 with calcium carbonate; (5) kaolinite from a commercial source (Santa Cruz Biotechnology, California, USA; Fig. 5d); (6) a tidal microbial mat bound to a microbially fertile mud underlayer (collected at the Barn Island saltmarsh, Connecticut, USA (41.3382° N, 71.8758° W) about 3–4 cm thick in total (Fig. 5d, f, overlain by sand and silt, respectively; and (7) commercial glass beads 212–300 μm, manufactured by Potters Industries LLC, Philadelphia, USA (capping layer in Fig. 5b, c, & d). As detailed in Table 2, these sediments were interlayered with artificial borosilicate glass sand in some of the experiments. Sand overlying clay, although gently introduced by sprinkling, formed ball-and-pillow/flame structures (Fig. 5c).

Methods

Experiments S1–S7 were designed to investigate the role of increasing salinity. Sediments were allowed to settle in 150 ml of distilled water, which was gradually replaced with artificial seawater (salinity

Table 2. *Experimental conditions*

Experiment	Sodium montmorillonite	Estuary mud*, glass sand	Glass sand, calcium montmorillonite	Glass sand, calcium montmorillonite + $CaCO_3$	Microbial mat, glass sand	Microbial mat, sterile estuary mud	Kaolinite	
Salinity	**S1**[†] 50 g clay	**S2#** 80 g sand 40 g mud 40 g sand	**S3#** 80 g sand 40 g clay 40 g sand	**S4#** 40 g sand 10 + 30 g $CaCO_3$ + clay 40 g sand	**S5#** 40 g sand Mat disc	**S6#** 40 g mud Mat disc	**S7#** 60 g clay	
Vibration	**V8**[†] 50 g clay	**V9** 40 g sand 20 g mud 40 g sand	**V10** 40 g sand 20 g clay 40 g sand	**V11** 40 g sand 5 + 15g $CaCO_3$ + clay 40 g sand	**V12** 40 g sand Mat disc	**V13** 40 g mud Mat disc	**V14** 30 g clay	
Loading					**L15**[†] 40 g sand Mat disc	**L16**[†] 40 g mud Mat disc		
Control (no action)	**C17**[†] 50 g clay	**C18** 40 g sand 20 g mud 40 g sand	**C19** 40 g sand 20 g clay 40 g sand	**C20** 40 g sand 5 + 15g $CaCO_3$ + clay 40 g sand	**C21** 40 g sand Mat disc	**C22** 40 g mud Mat disc	**C23** 30 g clay	
Unplanned microbial growth on kaolinite							**M24, M25** 60 g clay 100 ml DI	**M26** 60 g clay[†] 100 ml DI

Artificial seawater used (35% salinity), except in salinity experiments. Experiments carried out in glass jar = 150 ml water unless stated otherwise. See Figure 5 for photographs of sediment types and configurations.
*Sterilized in autoclave.
[†]Plastic container = 150 ml water.
[#]Glass conical flask = 500 ml water.

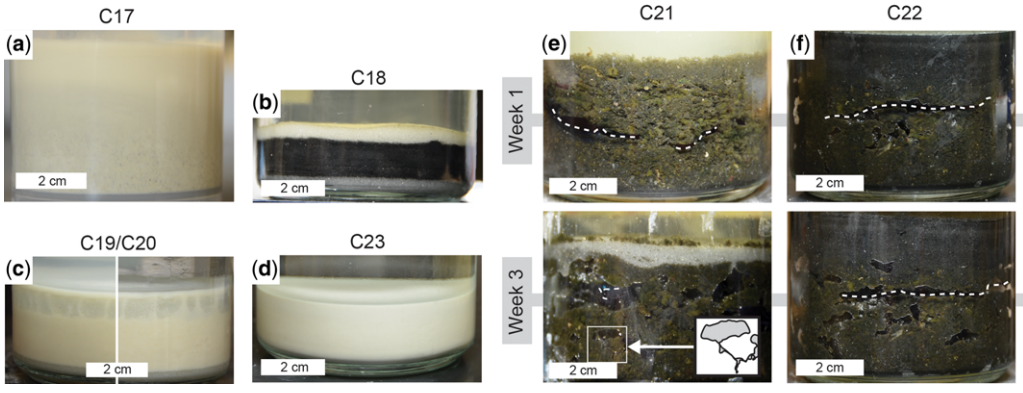

Fig. 5. Control experiments. All sediments were deposited as gently as possible under artificial seawater. See Table 2 for the sediment configurations designated by the alphanumeric codes. (**a**) Sodium montmorillonite. (**b**) Estuarine silty mud and glass sand. (**c**) Glass sand and calcium montmorillonite (left); glass sand and calcium montmorillonite mixed with calcium carbonate (right). (**d**) Kaolinite. (**e**, **f**) Controls for the experiments involving microbial mats (and underlying mud) with (e) overlying glass sand and (f) overlying estuarine silty mud. These sediments produced gas-filled voids without any experimental manipulation. Dashed white lines indicate the positions of voids inherited from the first few days. (e, inset) Sketch of hairline cracks running between gas voids in the area indicated by a square.

35‰). In the first three weeks, 1 ml of water was replaced every three days; subsequently, 10 ml of water was replaced every three days. Artificial seawater was used throughout in all other experiments. Experiments V8–V14 were designed to investigate the role of seismic vibrations. Flasks of sediment were vibrated using a VWR Analog Vortexer Mixer at a frequency of 900 rpm and an amplitude of *c.* 5 mm for 10 s in the horizontal plane and 10 s in the vertical plane. Experiments L15 and L16 were designed to investigate the role of loading or compaction. Iron filings (250 g) sealed in a plastic bag were gently lowered onto the sediment column after one week and then once more after another week. Experiments C17–C23 were control experiments in which the same sediments were left undisturbed.

The contribution of microbial processes was investigated by including a mat-bound, microbially stiffened mud among the sediments tested (sediment type E; experiments 5, 6, 12, 13, 15, 16, 21 and 22). This material was freshly collected from the field and was wet with seawater and highly cohesive; instead of being poured into the experimental vessels, it had to be cut to size with a scalpel and gently lowered and pushed into place. Microbial proliferation also occurred unexpectedly in a jar of kaolinite in distilled water, subsequently designated experiment 24. Experiments 25 and 26, the latter with sterilized kaolinite, were conducted in response as a *post hoc* replicate and control. With the exception of the estuarine mud (sediment type B) and the kaolinite in experiment 26, the investigated sediments were not previously sterilized.

Experiments were conducted either in conical flasks or (where sonication, centrifugation, vibration or loading were used) in sturdier glass or plastic beakers. All vessels were initially sterile. The experiments ran for four weeks and were monitored daily for crack formation and photographed weekly.

Results and discussion

Salinity. In agreement with previous work, our experiments showed that sodium montmorillonite, when allowed to settle in a closed vessel of distilled water (Fig. 6a), developed planar horizontal cracks a few centimetres below the sediment–water interface within hours of the addition of artificial seawater (experiment S1, Fig. 6b). In common with Burst (1965), we found that small vertical or oblique cracks opened secondarily at the edges of these planes, dividing the clay into tablets that parted slightly before reuniting, creating horizontal and vertical planes of discontinuity that reopened briefly if the vessel was nudged (or vibrated). The first set of cracks closed between three and four weeks into our experiment. After we substantially increased the salinity again (see Methods), a second set of cracks opened about 3 cm below the first (Fig. 6c). The control experiment (experiment S17; Fig. 5a) showed that the same clay did not crack when deposited directly under the same artificial seawater without any gradual change in salinity, confirming that an increase in salinity caused the observed cracking. We were unable to induce visible cracking by a change in salinity in the other materials tested (experiments S2–S7; not illustrated); the amount

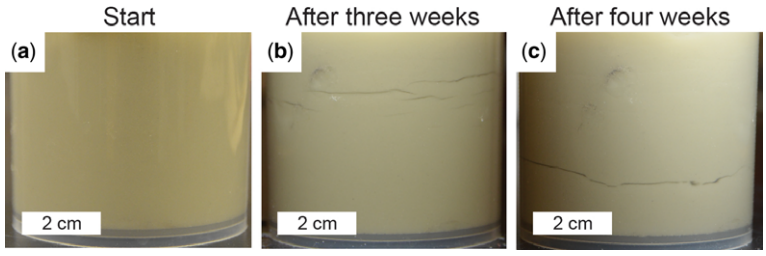

Fig. 6. Sodium montmorillonite with subaqueous cracks formed by increasing salinity (experiment S1). (**a**) Clay without cracks in distilled water prior to the addition of seawater. (**b**, **c**) Two generations of planar horizontal cracks produced by the addition of artificial seawater.

of added seawater might have been too small in the absence of sodium montmorillonite, which has a very high swelling capacity. We did not test the effect of a reduction in salinity.

Loading. The effect of loading was only tested on the mat-bound microbial mud because none of the other sediments was stiff enough to hold weight without flowing. These mats gradually produced gas bubbles, which formed gas-filled cavities in the sediment over four weeks. However, each addition of weights immediately squeezed gas out of the mats and produced an eruption of bubbles. The passage of these bubbles left irregular branching cavities behind in the mud (Fig. 7). Some of these cavities filled with sand from the overlying layer (Fig. 7b). Although these cavities were roughly tubular rather than planar and did not resemble cracks, it is possible that they could evolve into cracks during later compaction. It was notable that the gas voids produced by loading were more vertically oriented than those produced under other conditions, probably reflecting either the upwards trajectory of the escaping gas or a degree of lateral tension arising from vertical compression.

Vibration. We found that vibration caused nearly complete density inversion in the sediment columns (Fig. 8a–c), except when the stiff microbial mat and associated mud acted as a barrier to the downward transport of sand (as in experiment V12; Fig. 8d). However, the mud did not crack. Where sand had formed ball-and-pillow structures underlying clay (experiments V10 and V11), vibration caused the sand fingers to move through the clay until all the sand accumulated at the base of the vessel, except for isolated tendrils and blobs (Fig. 8b, c, insets). Vibration also dramatically accelerated the degassing of the microbial mats. We found that vibration had no effect on sodium montmorillonite or kaolinite, except to re-suspend them (experiments V8 and V14; not illustrated). Although we were not able to initiate sediment cracking using this simple approach, further experimental work using stiffer muds and more realistic simulations of seismic motion is motivated.

Microbial processes. The microbial mat (sediment type E; experiments 5, 6, 12, 13, 15, 16, 21 and 22) constantly produced pungent gases and caused loose flocs of mud to rise to the top of the water column, including in the control experiment. Much of the gas was retained in the sediment column, forming irregular cavities that only rarely filled with water or sediment (Figs 5e, f & 7). Removing the lids did not cause a pop or any effervescence, indicating that the overpressure was minor. Overlying sand passively filled the voids in some experiments (e.g. Fig. 7b). Hairline fractures were observed between some of the gas voids adjacent to the walls of the container (Fig. 5e, inset).

Additional evidence of microbially-induced cracking was discovered serendipitously in our laboratory. It was found that seven days after settling in distilled water (100 ml) in a sealed jar, kaolinite (60 g) spontaneously developed a *c.* 1 mm thick cyanobacteria-dominated microbial mat at the sediment–water interface, despite neither cyanobacteria nor any nutrient having been deliberately introduced (experiment M24). For unknown reasons, the undisturbed mat spontaneously formed small, radiating shrinkage cracks at the centre of the vessel over the following several days (Fig. 9a). To our knowledge, this is the first time that bacteria have been directly observed to mediate the formation of subaqueous sedimentary cracks. The mat was strong enough to peel back from the underlying sediment with tweezers (Fig. 9a, inset) and was revealed by microscopy to contain kaolinite grains interwoven with *Anabaena*-like cyanobacterial filaments (Fig. 9b, c). The experiment produced the same result when subsequently repeated under identical conditions (experiment M25; Fig. 9d), perhaps indicating that the clay stock was contaminated, whereas a sterile (autoclaved) control did not develop either a cohesive surface, cracks nor any other feature

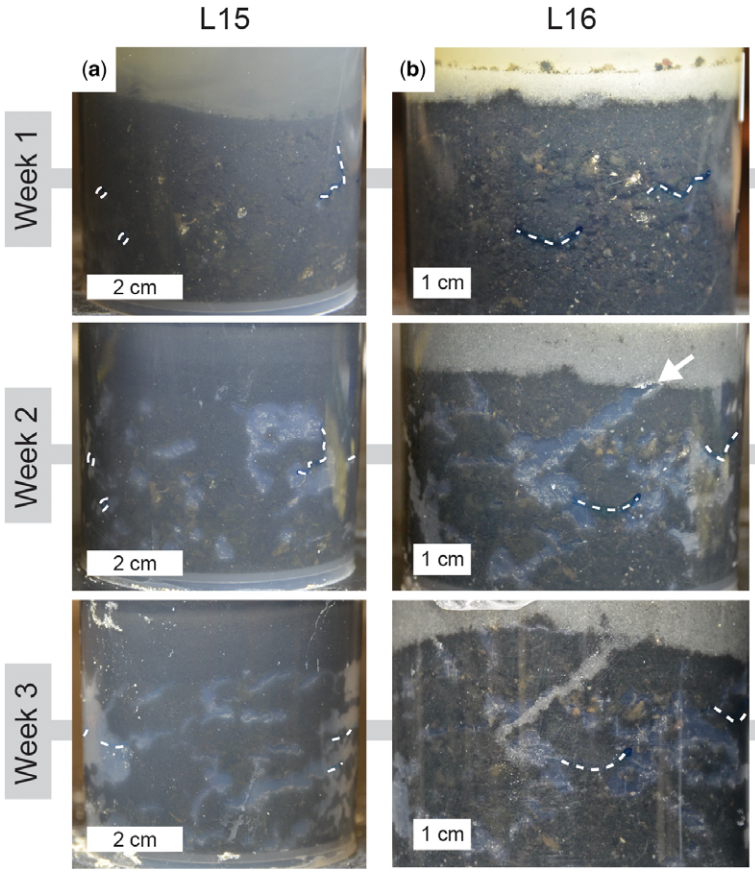

Fig. 7. Subaqueous sedimentary structures resulting from microbial gas production under compression. See Table 2 for the sediment configurations designated by the alphanumeric codes. Gas-filled voids appear bluish. Dashed white lines indicate the positions of voids inherited from the first few days. Microbial mats were overlain by (**a**) estuarine silty mud (**b**) glass sand. Week 1 photographs were taken prior to the application of a 250 g weight; week 2 photographs were taken one week after the application of the weight; and week 3 photographs were taken one week after the application of an additional 250 g. The addition of weights produced the largest gas-filled voids seen in any of our experiments. In experiment L16 (b), an oblique gas-filled void formed at the mud–sand interface (arrowed) after the application of the first weight and was filled geopetally by overlying sand after the application of the second weight.

(experiment M26; Fig. 9e). Kaolinite from the same stock did not produce mats or cracks in the experiments involving salinity change or vibration (experiments S7 and V14), despite not having been sterilized.

Conclusions

The foregoing review and experimental contributions can be summarized as follows:

(1) In clay-rich marginal sediments, which require little else to make them cohesive, salinity fluctuation might promote shrinkage-cracking by deflocculation and/or intracrystalline de-watering. We have successfully replicated previous experiments showing that the latter mechanism is effective in producing small cracks several centimetres below the sediment–water interface, but more experimental work is needed. Geological evidence for salinity fluctuation in cracked sediments is limited. In particular, low ichnodiversity is equivocal.

(2) In high-energy sediments, burial compaction, loading and wave stress might cause cracking by (a) increasing cohesion by de-watering and grain reorientation, (b) inducing

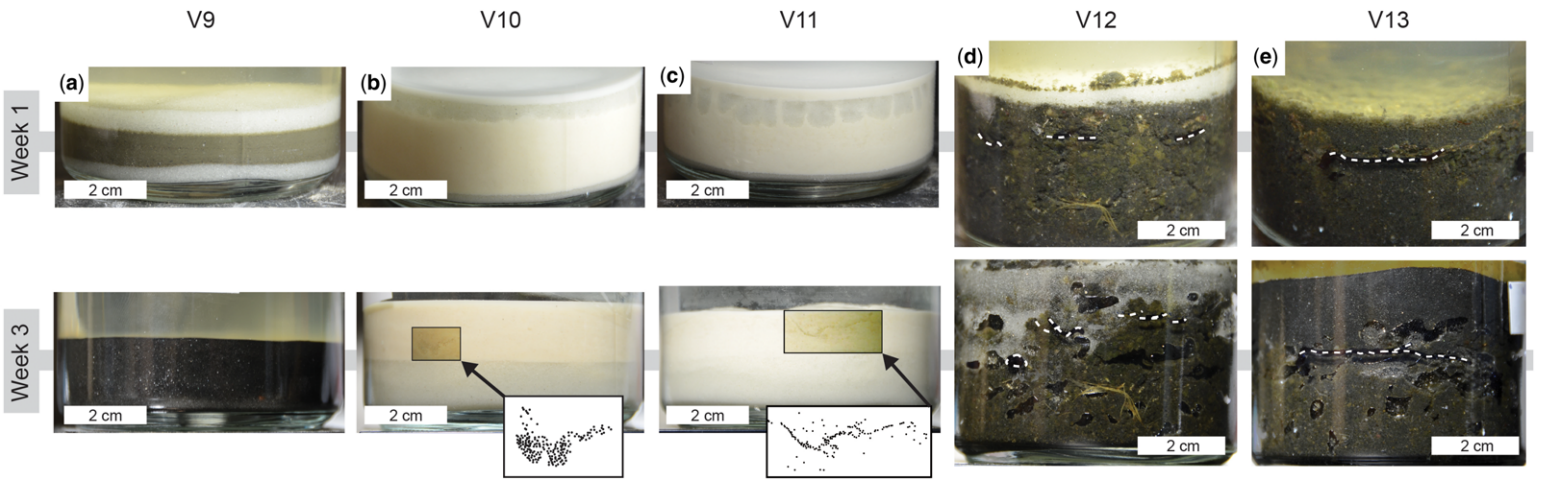

Fig. 8. Results of the vibration of subaqueous sediment. See Table 2 for the sediment configurations designated by the alphanumeric codes. Rapid vibration was applied on two orthogonal axes to simulate seismic shaking. Week 1 photographs were taken prior to the application of any vibration. Week 3 photographs show sediments after two bouts of vibration separated by an interval of one week. (**a**) Sand overlying estuarine silty mud was transported to the base of the sediment column; any residue was not visible. Glass sand overlying (**b**) sodium montmorillonite and (**c**) calcium montmorillonite mixed with calcium carbonate was mostly transported to the base of the sediment column, but left wispy structures behind in the clay (highlighted and shown in insets). (**d**) Glass sand and **(e)** estuarine silty mud overlying microbial mats penetrated some distance downwards under vibration. Vibration also accelerated the escape of gas bubbles, leaving behind voids filled with water rather than gas. Dashed white lines indicate the positions of voids inherited from the first few days. Note small piece of grass in (d).

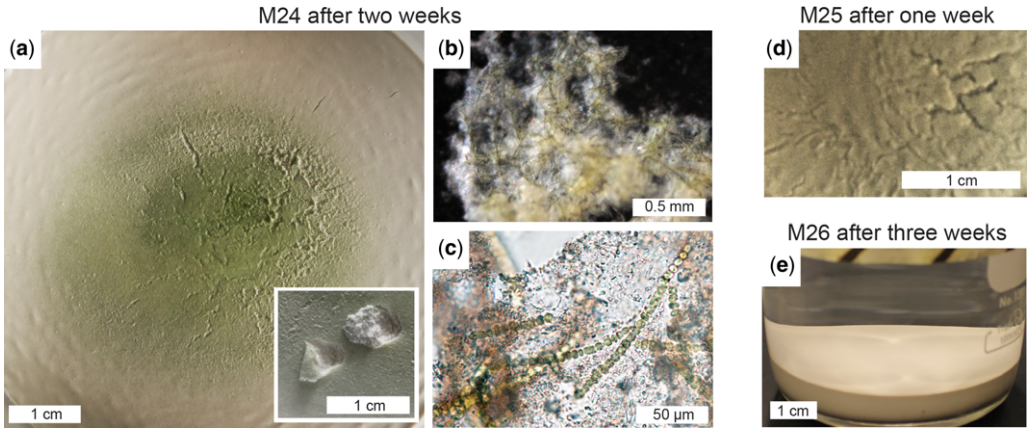

Fig. 9. Subaqueous cracks developed during experiments in biostabilized kaolinite. See Table 2 for the sediment configurations designated by the alphanumeric codes. (**a**) Underwater photograph of kaolinite undisturbed for two weeks in distilled water. Note greenish hue, small concentric wrinkles and fine radiating cracks. Inset: The surface layer can be pulled away as a cohesive, 0.5 mm thick green sheet. (**b**) Reflected light micrograph showing interwoven green cyanobacterial filaments binding the clay particles together. (**c**) Transmitted light micrograph confirming a monospecific *Anabaena*-like cyanobacterial population. (**d**) Underwater photograph of branching cracks and irregular surface developed in a duplicate experiment. (**e**) No crack or other surface feature developed if the kaolinite–water mixture was sterilized in an autoclave at the beginning of the experiment.

shrinkage-cracking by de-watering and (c) opening mechanical (diastasis) cracks in stiff sediments without shrinkage. There is good geological evidence for diastasis cracking, but sand-filled cracks are only rarely associated with load structures. Liquefaction and sand injection features are associated with some cracks, but could also reflect seismicity. In our experiments, we found that the addition of weights to the sediment column did not crack microbial mud, but may have affected the orientation of gas voids and their chances of being filled with sand.

(3) In tectonically suitable settings, seismic activity might cause cracking by (a) increasing cohesion by de-watering and grain reorientation, (b) inducing shrinkage-cracking by de-watering and (c) opening mechanical cracks in stiff sediments without shrinkage. Geological evidence includes the laterally extensive occurrence of molar tooth cracks in some settings. Liquefaction and sand injection features are associated with some cracks, but do not necessarily imply seismicity. There is no experimental evidence for the seismicity hypothesis and, in our vibration experiments, unconsolidated subaqueous clay was seen to flow rather than to crack, whereas biostabilized mud did not crack. It remains plausible that a clay layer, if first made cohesive, could then be induced to crack by seismic motion.

(4) Microbial processes might cause cracking by (a) stiffening mud and sand by biostabilization, (b) producing disruptive gases and (c) inducing volume change by organic decay. Experimental evidence is so far limited to the cracking of thin mats at the sediment–water interface in clay (this paper) and the generation of molar-tooth-like cavities by microbial gas (Furniss *et al.* 1998). Geological evidence includes the presence of cracks in pure sandstones, a common association with MISS, and carbon isotope evidence. Subseafloor microbial gas voids in the Baltic Sea resemble some intrastratal cracks (Abegg & Anderson 1997).

(5) Diagenetic processes might cause cracking below the sediment–water interface by (a) stiffening sediment through authigenic cementation and (b) inducing volume change through mineralogical phase changes. There is no experimental evidence for this hypothesis. Geological evidence includes the common presence of carbonate cements in cracked siliciclastic sediments as well as evidence for phase changes in Proterozoic carbonates.

Individually, none of these mechanisms can be reconciled to every set of subaqueous cracks in the geological record. The evidence suggests that different mechanisms have induced cracking under different circumstances. Consequently, unlike desiccation cracks, neither the presence nor the absence of

subaqueous cracks furnishes an immediate palaeoenvironmental interpretation. To explain the formation of cracks in any particular instance, two questions must be answered: (1) why did subaqueous sediment particles cohere rather than shift around each other; and (2) once the sediment was sufficiently cohesive, how was it stressed to the point of brittle failure? Possible answers to the first question include the physicochemical attraction between clay particles, microbial biostabilization and early diagenetic cementation. Possible answers to the second question include microbial gas production, lateral tension resulting from gravitational compaction, seismic disturbance, wave action, mineralogical phase change and salinity fluctuation. Further experimental work to investigate all of these processes is clearly motivated.

Further light may be shed on the causes of subaqueous cracking by the investigation of possible secular trends in its occurrence and facies distribution. MTS are restricted to pre-Cryogenian carbonates; their disappearance has been ascribed to a decrease in carbonate precipitation in the mid-Proterozoic, resulting either from a falling saturation state or from increasing chemical inhibition (Shields 2002; Higgins *et al.* 2009). Precambrian–Cambrian strata contain subaqueous cracks formed in a variety of palaeobathymetric settings, whereas in younger strata such cracks tend to be limited to shoreline and lacustrine settings (Table 1). This has been regarded as a primary, genuine trend rather than an artefact of preservation or sampling bias (Pratt 1998*a*). We suggest that the trend, if it is real, is most likely to reflect biogeochemically influenced changes in sediment stiffness across space and time. The traditional view that microbial mats were markedly less abundant after the onset of metazoan grazing has recently been called into question (Davies *et al.* 2016). However, there is good evidence that marine muds were much more coherent prior to the development of a bioturbated mixed layer, which did not begin to approach its current thickness until at least the Late Silurian (Tarhan *et al.* 2015). A fuller understanding of subaqueous sedimentary cracks may ultimately inform our understanding of the rheological and biogeochemical evolution of sediments through time.

SM is supported through a Yale Postdoctoral Associateship by the NASA Astrobiology Institute (NNA13AA90A; Foundations of Complex Life, Evolution, Preservation and Detection on Earth and Beyond) and thanks the Brasier group for fruitful discussion in Oxford. AvSH is supported by a NASA Astrobiology Institute Postdoctoral Fellowship. DMc recognizes the support of an NSERC discovery grant. We thank Holger Petermann for translating into English Jüngst's 1934 paper on synaeresis (translation available from SM on request) and Stefan Nicolescu of the Yale Peabody Museum for supplying Figure 2a. We thank C.A. Cowan for generous and interesting discussion. The reviews of Alex Brasier, Tony Prave and one anonymous reviewer are recognized with thanks.

References

Abegg, F. & Anderson, A.L. 1997. The acoustic turbid layer in muddy sediments of Eckernfoerde Bay, Western Baltic: methane concentration, saturation and bubble characteristics. *Marine Geology*, **137**, 137–147.

Allen, P.A. & Leather, J. 2006. Post-Marinoan marine siliciclastic sedimentation: the Masirah bay formation, Neoproterozoic Huqf Supergroup of Oman. *Precambrian Research*, **144**, 167–198.

Anketell, J.M., Cegla, J. & Dzulynski, S. 1970. On the deformational structures in systems with reversed density gradients. *Rocznik Polskiego Towarzystwa Geologicznego*, **40**, 3–29.

Assereto, R.L.A.M. & Kendall, G.St.C. 1977. Nature, origin and classification of peritidal tepee structures and related breccias. *Sedimentology*, **24**, 153–210.

Astin, T.R. 1986. Septarian crack formation in carbonate concretions from shales and mudstones. *Clay Minerals*, **21**, 617–631.

Beukes, N.J. 1984. Sedimentology of the Kuruman and Griquatown iron-formations, Transvaal Supergroup, Griqualand West, South Africa. *Precambrian Research*, **24**, 47–84.

Bhattacharya, J.P. & MacEachern, J.A. 2009. Hyperpycnal rivers and prodeltaic shelves in the Cretaceous seaway of North America. *Journal of Sedimentary Research*, **79**, 184–209, https://doi.org/10.2110/jsr.2009.026

Bishop, J.W., Sumner, D.Y. & Huerta, N.J. 2006. Molar tooth structures of the Neoarchean Monteville Formation, Transvaal Supergroup, South Africa. II: a wave-induced flow model. *Sedimentology*, **53**, 1069–1082.

Buatois, L.A., Saccavino, L.L. & Zavala, C. 2011. Ichnologic signatures of hyperpycnal flow deposits in Cretaceous river-dominated deltas, Austral Basin, southern Argentina. *In*: Slatt, R.M. & Zavala, C. (eds) *Sediment Transfer from Shelf to Deep Water – Revisiting the Delivery System*. AAPG Studies in Geology, **61**, 153–170.

Burst, J.F. 1965. Subaqueously formed shrinkage cracks in clay. *Journal of Sedimentary Research*, **35**, 348–353, https://doi.org/10.1306/74D71271-2B21-11D7-8648000102C1865D

Calver, C.R. & Baillie, P.W. 1990. Early diagenetic concretions associated with intrastratal shrinkage cracks in an Upper Proterozoic dolomite, Tasmania, Australia. *Journal of Sedimentary Research*, **60**, 293–305, https://doi.org/10.1306/212F9179-2B24-11D7-8648000102C1865D

Carroll, A.R. & Wartes, M.A. 2003. Organic carbon burial by large Permian lakes, northwest China. *In*: Chan, M.A. & Archer, A.W. (eds) *Extreme depositional environments: mega end members in geologic time*. Geological Society of America, Special Papers, **370**, 91–104, https://doi.org/10.1130/0-8137-2370-1.91

Cazier, E.C., Hein, M. & Pemberton, S.G. 2011. Sedimentology of Early Aptian Reservoir, Dunga Field, Kazakhstan. Search and Discovery Article, **#50394**.

Chakraborty, P.P., Das, P.S.S., Das, K., Mishra, S.R. & Paul, P. 2012. Microbial mat related structures (MRS) from Mesoproterozoic Chhattisgarh and Khariar basins, Central India and their bearing on shallow marine sedimentation. *Episodes*, **35**, 513–523.

Chen, J., Chough, S.K., Chun, S.S. & Han, Z. 2009. Limestone pseudoconglomerates in the Late Cambrian Gushan and Chaomidian Formations (Shandong Province, China): soft-sediment deformation induced by storm-wave loading. *Sedimentology*, **56**, 1174–1195.

Clemmey, H. 1978. A Proterozoic lacustrine interlude from the Zambian Copperbelt. *In*: Matter, A. & Tucker, M.E. (eds) *Modern and Ancient Lake Sediments*. Blackwell, Oxford, 259–278.

Cook, H.E. & Taylor, M.E. 1977. Comparison of continental slope and shelf environments in the Upper Cambrian and Lowest Ordovician of Nevada. *In*: Cook, H.E. & Enos, P. (eds) *Deep-Water Carbonate Environments*. Society of Economic Paleontologists and Mineralogists, Special Publications, **25**, 51–81.

Cowan, C.A. & James, N.P. 1992. Diastasis cracks: mechanically generated synaeresis-like cracks in Upper Cambrian shallow water oolite and ribbon carbonates. *Sedimentology*, **39**, 1101–1118.

Davies, N.S., Liu, A.G., Gibling, M.R. & Miller, R.F. 2016. Resolving MISS conceptions and misconceptions: a geological approach to sedimentary surface textures generated by microbial and abiotic processes. *Earth-Science Reviews*, **154**, 210–246.

De Morton, S. 2011. *The Neoproterozoic carbonate sediments of the Trezona Formation, Central Flinders Ranges, South Australia*. Honours thesis, University of Melbourne.

De Deckere, E.M.G.T., Tolhurst, T.J. & De Brouwer, J.F.C. 2001. Destabilization of cohesive intertidal sediments by infauna. *Estuarine, Coastal and Shelf Science*, **53**, 665–669.

Donovan, R.N. & Foster, R.J. 1972. Subaqueous shrinkage cracks from the Caithness Flagstone Series (middle Devonian) of northeast Scotland. *Journal of Sedimentary Research*, **42**, 309–317, https://doi.org/10.1306/74D72531-2B21-11D7-8648000102C1865D

Duck, R.W. 1995. Subaqueous shrinkage cracks and early sediment fabrics preserved in Pleistocene calcareous concretions. *Journal of the Geological Society, London*, **152**, 151–156, https://doi.org/10.1144/gsjgs.152.1.0151

Eby, D.E. 1977. *Sedimentation and early diagenesis within eastern portions of the 'Middle Belt Carbonate Interval' (Helena Formation), Belt Supergroup (Precambrian Y), western Montana*. PhD thesis, State University of New York.

Eoff, J.D. 2014. Suspected microbial-induced sedimentary structures (MISS) in Furongian (Upper Cambrian; Jiangshanian, Sunwaptan) strata of the Upper Mississippi Valley. *Facies*, **60**, 801–814.

Fairchild, I.J. 1980. Sedimentation and origin of a late Precambrian 'dolomite' from Scotland. *Journal of Sedimentary Research*, **50**, 423–446.

Fairchild, I.J. & Hambrey, M.J. 1984. The Vendian succession of northeastern Spitsbergen: petrogenesis of a dolomite–tillite association. *Precambrian Research*, **26**, 111–167, https://doi.org/10.1016/0301-9268(84)90042-1

Fairchild, I.J., Einsel, G. & Song, T. 1997. Possible seismic origin of molar tooth structures in Neoproterozoic carbonate ramp deposits, north China. *Sedimentology*, **44**, 611–636, https://doi.org/10.1046/j.1365-3091.1997.d01-40.x

Fielding, C.R., Bann, K.L., MacEachern, J.A., Tye, S.C. & Jones, B.G. 2006. Cyclicity in the nearshore marine to coastal, Lower Permian, Pebbley Beach Formation, southern Sydney Basin, Australia: a record of relative sea-level fluctuations at the close of the Late Palaeozoic Gondwanan ice age. *Sedimentology*, **53**, 435–463.

Frank, T.D. & Lyons, T.W. 1998. 'Molar-tooth' structures: a geochemical perspective on a Proterozoic enigma. *Geology*, **26**, 683–686.

Furniss, G., Rittel, J.F. & Winston, D. 1998. Gas bubble and expansion crack origin of 'molar-tooth' calcite structures in the middle Proterozoic Belt Supergroup, western Montana. *Journal of Sedimentary Research*, **68**, 104–114, https://doi.org/10.2110/jsr.68.104

Gehling, J.G. 1999. Microbial mats in terminal Proterozoic siliciclastics: Ediacaran death masks. *Palaios*, **14**, 40–57.

Gehling, J.G. 2000. Environmental interpretation and a sequence stratigraphic framework for the terminal Proterozoic Ediacara Member within the Rawnsley Quartzite, South Australia. *Precambrian Research*, **100**, 65–95, https://doi.org/10.1016/S0301-9268(99)00069-8

Giddings, J.A., Wallace, M.W. & Woon, E.M.S. 2009. Interglacial carbonates of the Cryogenian Umberatana Group, northern Flinders Ranges, South Australia. *Australian Journal of Earth Sciences*, **56**, 907–925, https://doi.org/10.1080/08120090903005378

Halverson, G.P., Maloof, A.C. & Hoffman, P.F. 2004. The Marinoan glaciation (Neoproterozoic) in northeast Svalbard. *Basin Research*, **16**, 297–324.

Harazim, D., Callow, R.H. & McIlroy, D. 2013. Microbial mats implicated in the generation of intrastratal shrinkage ('synaeresis') cracks. *Sedimentology*, **60**, 1621–1638, https://doi.org/10.1111/sed.12044

Harris, C.W. & Eriksson, K.A. 1990. Allogenic controls on the evolution of storm to tidal shelf sequences in the Early Proterozoic Uncompahgre Group, southwest Colorado, USA. *Sedimentology*, **37**, 189–213.

Harwood, C.L. & Sumner, D.Y. 2011. Microbialites of the Neoproterozoic Beck Spring Dolomite, southern California. *Sedimentology*, **58**, 1648–1673.

Higgins, J.A., Fischer, W.W. & Schrag, D.P. 2009. Oxygenation of the ocean and sediments: consequences for the seafloor carbonate factory. *Earth and Planetary Science Letters*, **284**, 25–33.

Hoffman, P.F. & Macdonald, F.A. 2010. Sheet-crack cements and early regression in Marinoan (635 Ma) cap dolostones: regional benchmarks of vanishing ice-sheets? *Earth and Planetary Science Letters*, **300**, 374–384.

Hood, A.v.S. & Wallace, M.W.W. 2012. Synsedimentary diagenesis in a Cryogenian reef complex: ubiquitous marine dolomite precipitation. *Sedimentary Geology*, 255–256, 56–71.

Hood, A.v.S., Wallace, M.W., Reed, C.P., Hoffmann, K.-H. & Freyer, E.E. 2015. Enigmatic carbonates of the Ombombo Subgroup, Otavi Fold Belt, Namibia: a

prelude to extreme Cryogenian anoxia? *Sedimentary Geology*, **324**, 12–31, https://doi.org/10.1016/j.sedgeo.2015.04.007

Horodyski, R.J. 1976. Stromatolites of the Upper Siyeh Limestone (Middle Proterozoic), Belt Supergroup, Glacier National Park, Montana. *Precambrian Research*, **3**, 517–536.

Hsiao, L.Y., Graham, S.A. & Tilander, N. 2010. Stratigraphy and sedimentation in a rift basin modified by synchronous strike-slip deformation: southern Xialiao Basin, Bohai, offshore China. *Basin Research*, **22**, 61–78.

Hughes, N.C. & Hesselbo, S.R. 1997. Stratigraphy and sedimentology of the St. Lawrence Formation. Upper Cambrian of the northern Mississippi Valley. *Contributions in Biology & Geology*, **91**, 1–50.

James, N.P., Narbonne, G.M. & Sherman, A.G. 1998. Molar-tooth carbonates: shallow subtidal facies of the Mid-to Late Proterozoic. *Journal of Sedimentary Research*, **68**, 716–722.

Jiang, G., Kennedy, M.J., Christie-Blick, N., Wu, H. & Zhang, S. 2006. Stratigraphy, sedimentary structures, and textures of the late Neoproterozoic Doushantuo cap carbonate in South China. *Journal of Sedimentary Research*, **76**, 978–995.

Jirsa, M. & Fralick, P.W. 2010. Field trip 4: geology of the Gunflint Iron Formation and the Sudbury Impact Layer. *Precambrian Research Center Guidebook*, **10-01**, 77–92.

Jüngst, H. 1934. Zur geologischen Bedeutung der Synärese. *Geologische Rundschau*, **25**, 312–325.

Kidder, D.L. 1990. Facies-controlled shrinkage-crack assemblages in Middle Proterozoic mudstones from Montana, USA. *Sedimentology*, **37**, 943–951, https://doi.org/10.1111/j.1365-3091.1990.tb01836.x

Kuang, H.-W. 2014. Review of molar tooth structure research. *Journal of Palaeogeography*, **3**, 359–383.

Lanés, S., Giambiagi, L., Bechis, F. & Tunik, M. 2008. Late Triassic–Early Jurassic successions of the Atuel depocenter: sequence stratigraphy and tectonic controls. *Revista de la Asociación Geológica Argentina*, **63**, 534–548.

Lévéille, R.J., Fyfe, W.S. & Longstaffe, F.J. 2000. Unusual secondary Ca–Mg-carbonate-kerolite deposits in Basaltic Caves, Kauai, Hawaii. *The Journal of Geology*, **108**, 613–621.

Marek, S.G. 2015. *A stratigraphic framework for Late Cambrian–Early Ordovician carbonate slope to basinal sediments in Tybo Canyon, Hot Creek Range, Nevada*. Thesis, Texas A&M University.

McIlroy, D. 2004. Ichnofabrics and sedimentary facies of a tide-dominated delta: Jurassic Ile Formation of Kristin Field, Haltenbanken, offshore Mid-Norway. *In*: McIlroy, D. (ed.) *The Application of Ichnology to Stratigraphic and Palaeoenvironmental Analysis*. Geological Society, London, Special Publications, **228**, 237–272, https://doi.org/10.1144/GSL.SP.2004.228.01.12

Menon, L.R., McIlroy, D., Liu, A.G. & Brasier, M.D. 2016. The dynamic influence of microbial mats on sediments: fluid escape and pseudofossil formation in the Ediacaran Longmyndian Supergroup, UK. *Journal of the Geological Society, London*, **173**, 177–185, https://doi.org/10.1144/jgs2015-036

Morrow, D.W. 1972. An injection structure in a Permian Limestone, northern British Columbia. *Journal of Sedimentary Petrology*, **42**, 230–235.

Mörz, T., Karlik, E.A., Kreiter, S. & Kopf, A. 2013. An experimental setup for fluid venting in unconsolidated sediments: new insights to fluid mechanics and structures. *Sedimentary Geology*, **196**, 251–267.

Owen, G. 1996. Experimental soft-sediment deformation structures formed by the liquefaction of unconsolidated sands and some ancient examples. *Sedimentology*, **43**, 279–293.

Patel, S.J., Joseph, J.K. & Bhatt, N.Y. 2013. Facies controlled synaeresis cracks in mixed siliciclastic–carbonate sediments of Middle Jurassic of Patcham Island, Kachchh, Western India. *Journal of the Geological Society of India*, **82**, 9–14.

Pflueger, F. 1999. Matground structures and redox facies. *Palaios*, **14**, 25–39.

Plummer, P.S. & Gostin, V.A. 1981. Shrinkage cracks: desiccation or synaeresis? *Journal of Sedimentary Research*, **51**, 1147–1156, https://doi.org/10.1306/212F7E4B-2B24-11D7-8648000102C1865D

Pomoni-Papaioannou, F. & Karakitsios, V. 2002. Facies analysis of the Trypali carbonate unit (Upper Triassic) in central-western Crete (Greece): an evaporite formation transformed into solution-collapse breccias. *Sedimentology*, **49**, 1113–1132.

Porada, H. & Druschel, G. 2010. Evidence for participation of microbial mats in the deposition of the siliciclastic 'ore formation' in the Copperbelt of Zambia. *Journal of African Earth Sciences*, **58**, 427–444.

Pratt, B.R. 1998*a*. Syneresis cracks: subaqueous shrinkage in argillaceous sediments caused by earthquake-induced dewatering. *Sedimentary Geology*, **117**, 1–10, https://doi.org/10.1016/S0037-0738(98)00023-2

Pratt, B.R. 1998*b*. Molar-tooth structure in Proterozoic carbonate rocks: origin from synsedimentary earthquakes, and implications for the nature and evolution of basins and marine sediment. *Geological Society of America Bulletin*, **110**, 1028–1045.

Pratt, B.R. 2001. Septarian concretions: internal cracking caused by synsedimentary earthquakes. *Sedimentology*, **48**, 189–213, https://doi.org/10.1046/j.1365-3091.2001.00366.x

Raiswell, R. 1971. The growth of Cambrian and Liassic concretions. *Sedimentology*, **17**, 147–171.

Rodriguez-Blanco, J.D., Shaw, S. & Benning, L.G. 2011. The kinetics and mechanisms of amorphous calcium carbonate (ACC) crystallization to calcite, via vaterite. *Nanoscale*, **3**, 265–271.

Rodriguez-Blanco, J.D., Shaw, S., Bots, P., Roncal-Herrero, T. & Benning, L.G. 2014. The role of Mg in the crystallization of monohydrocalcite. *Geochimica et Cosmochimica Acta*, **127**, 204–220.

Rossetti, D. de F. 1998. Facies architecture and sequential evolution of an incised-valley estuarine fill: the Cujupe Formation (Upper Cretaceous to ?Lower Tertiary), São Luís Basin, northern Brazil. *Journal of Sedimentary Research*, **68**, 299–310.

Schubel, K.A. & Simonson, B.M. 1990. Petrography and diagenesis of cherts from Lake Magadi, Kenya. *Journal of Sedimentary Petrology*, **60**, 761–776.

Shen, B., Dong, L. *et al.* 2016. Molar tooth carbonates and benthic methane fluxes in Proterozoic oceans. *Nature Communications*, **7**, 10317.

Shields, G.A. 2002. 'Molar-tooth microspar': a chemical explanation for its disappearance ~750 Ma. *Terra Nova*, **14**, 108–113.

Shinn, E.A. 1969. Submarine lithification of Holocene carbonates in the Persian Gulf. *Sedimentology*, **12**, 109–144.

Smith, A.G. 1968. The origin and deformation of some molar-tooth structures in the Precambrian Belt-Purcell Supergroup. *Journal of Geology*, **76**, 426–443.

Tanner, P.W.G. 1998. Interstratal dewatering origin for polygonal patterns of sand-filled cracks: a case study from late Proterozoic metasediments of Islay, Scotland. *Sedimentology*, **45**, 71–89.

Tanner, P.W.G. 2003. Syneresis. *In*: Middleton, G.V. (ed.) *Encyclopedia of Sediments and Sedimentary Rocks*. Kluwer Academic, Dordrecht, 718–720.

Tarhan, L.G., Droser, M.L., Planavsky, N.J. & Johnston, D.T. 2015. Protracted development of bioturbation through the early Palaeozoic Era. *Nature Geoscience*, **8**, 865–869.

Timms, N.E., Olierook, H.K.H., Wilson, M.E.J., Piane, C.D., Hamilton, P.J., Cope, P. & Stütenbecker, L. 2015. Sedimentary facies analysis, mineralogy and diagenesis of the Mesozoic aquifers of the central Perth Basin, Western Australia. *Marine and Petroleum Geology*, **60**, 54–78.

Törö, B., Pratt, B.R. & Renaut, R.W. 2013. Seismically induced soft-sediment deformation structures in the Eocene lacustrine Green River Formation (Wyoming, Utah, Colorado, USA) – a preliminary study. GeoConvention 2013, Integration: Geoscience Engineering Partnership, 6–12 May 2013, Calgary, AB, Canada.

Turner, E.C., James, N.P. & Narbonne, G.M. 1997. Growth dynamics of Neoproterozoic calcimicrobial reefs, Mackenzie Mountains, northwest Canada. *Journal of Sedimentary Research*, **67**, 437–450.

Van Houten, F.B. 1962. Cyclic sedimentation and the origin of analcime-rich Upper Triassic Lockatong Formation, west-central New Jersey and adjacent Pennsylvania. *American Journal of Science*, **260**, 561–576.

Van Leeuwen, N. 2013. *West Basin Lake: sediments, microbial formation and carbonate mineral precipitation*. Honours thesis, University of Melbourne.

White, W.A. 1961. Colloid phenomena in sedimentation of argillaceous rocks. *Journal of Sedimentary Research*, **31**, https://doi.org/10.1306/74D70BE6-2B21-11D7-8648000102C1865D

Winslow, M.A. 1983. Clastic dike swarms and the structural evolution of the foreland fold and thrust belt of the southern Andes. *Geological Society of America Bulletin*, **94**, 1073–1080.

Winston, D., Rittel, J.F. & Furniss, G. 1999. Gas bubble and expansion crack origin of molar-tooth calcite structures in the Middle Proterozoic Belt Supergroup, western Montana – Reply. *Journal of Sedimentary Research*, **69**, 1140–1145.

Xiaoying, S., Chuanheng, Z., Ganqing, J., Juan, L., Yi, W. & Dianbo, L. 2008. Microbial mats in the Mesoproterozoic carbonates of the North China platform and their potential for hydrocarbon generation. *Journal of China University of Geosciences*, **19**, 549–566.

Zaitlin, B.A., Dalrymple, R.W. & Boyd, R. 1994. The stratigraphic organization of incised-valley systems associated with relative sea-level change. *In*: Dalrymple, R.W., Boyd, R. & Zaitlin, B.A. (eds) *Incised-valley Systems: Origin and Sedimentary Sequences*. Society of Economic Paleontologists and Mineralogists, Special Publications, **51**, 45–60.

Zonneveld, J.-P., Gingras, M.K. & Pemberton, S.G. 2001. Trace fossil assemblages in a Middle Triassic mixed siliciclastic–carbonate marginal marine depositional system, British Columbia. *Palaeogeography, Palaeoclimatology, Palaeoecology*, **166**, 249–276.